Fault-Tolerant Control Strategies for a Class of Euler-Lagrange Nonlinear Systems Subject to Simultaneous Sensor and Actuator Faults

Maryam Abdollahi

A Thesis

in

The Department

of

Electrical and Computer Engineering

Presented in Partial Fulfillment of the Requirements

for the Degree of Master of Applied Science at

Concordia University

Montréal, Québec, Canada

December 2017

CONCORDIA UNIVERSITY

SCHOOL OF GRADUATE STUDIES

This is to certify that the thesis prepared

By: Maryam Abdollahi

Entitled: Fault-Tolerant Control Strategies for a Class of Euler-Lagrange Nonlinear Systems Subject to Simultaneous Sensor and Actuator Faults

and submitted in partial fulfilment of the requirements for the degree of

Master of Applied Science

complies with the regulations of this University and meets the accepted standards with respect to originality and quality.

Signed by the final examining committee:

_____ Dr. Rabin Raut, Chair

_____ Dr. Luis Rodrigues, Examiner

_____ Dr. Ali Dolatabadi, Examiner

_____ Dr. Kash Khorasani, Supervisor

Approved by: _____

Dr. W. E. Lynch, Chair

Department of Electrical and Computer Engineering

_____

Dr. A. Asif

Dean, Faculty of Engineering and Computer Science

Date: _____

ABSTRACT

Fault-Tolerant Control Strategies for a Class of Euler-Lagrange Nonlinear Systems Subject to Simultaneous Sensor and Actuator Faults

Maryam Abdollahi

The problem of Fault Detection, Isolation, and Estimation (FDIE) as well as Fault Tolerant Control (FTC) for a class of nonlinear systems modeled with Euler-Lagrange (EL) equations subjected to simultaneous sensor and actuator faults are considered in this study. To tackle this problem, first state and output linear transformations are introduced to decouple the effects of sensor and actuator faults. These transformations do not depend on the system nonlinearities. An analytical procedure based on two Linear Matrix Inequality (LMI) feasibility conditions is proposed to obtain these transformations.

Once, the effects of faults are decoupled, two Sliding Mode Observers (SMO) are designed to reconstruct each type of fault, separately. Subsequently, the results of fault estimations are fed back to the controller and the effects of faults are compensated for. In this study, the mathematical stability proof of the coupled controller, observers, and the nonlinear system is provided. Unlike previous methodologies in the literature, no limiting assumptions such as Lipschitz conditions are imposed on the system.

Next, a novel fault tolerant control scheme is proposed in which a single SMO is used to reconstruct sensor faults and provide a compensation term to rectify the effects of faults. However, to deal with actuator faults, a Sliding Mode Controller (SMC) is

employed. Using this robust FTC technique, zero tracking error in the presence of uncertainties, measurement noise, disturbances, and faults as well as estimation of the actuator faults are possible. The stability proof for the coupled nonlinear controller, observer and plant is provided by using the properties of Euler-Lagrange equations and sliding mode techniques. Finally, to evaluate the performance of the proposed FDIE and FTC approaches, extensive sets of simulations are performed on a 3 Degrees Of Freedom (DOF) Autonomous Underwater Vehicle (AUV). Simulation studies show the promising results obtained as a result of the presented approaches as compared to those obtained by using the existing methodologies.

ACKNOWLEDGEMENTS

I would like to express my gratitude to my supervisors Professor Kash Khorasani for the opportunity to join his research group at Concordia University and his patience and continuous support of my research. Moreover, I would also like to express my sincere gratitude and appreciation to Professor H.A. Talebi for his consistent guidance and motivation. This thesis could not be accomplished without his invaluable guidance and support.

I am also thankful to my friends and colleagues in System and Control Laboratory: Amir Baniamerian, Bahar Pourbabaee, Najmeh Daroogheh, Zahra Gallehdari, Arefeh Amrollahi, and Esmaeil Alizadeh for stimulating discussion and exchanges as well as providing a warm and supportive environment throughout these years. My sincere thanks also go to Elaheh Marzban, Sara Rahimifard, Raheleh Abdoli, Ideh Sarbishei, and Sahar Hoseingholizade for their kindness and emotional support through the difficult times.

Finally, I must express my deepest gratitude to my beloved ones in particular my parents Zahra and Alireza, and my sisters Farzaneh and Azadeh for their unconditional love and support. None of these would have been possible without their encouragement. This work is dedicated to them.

Table of Contents

List of Figures

List of Tables

Chapter 1

Introduction

Fault detection, isolation and estimation have received a great deal of attention over the past two decades, due to the increasing demand on reliability, safety of technical plants and their components as well as reducing the maintenance cost and risk of catastrophic failures. Considering the model of the system, that of the affected fault and the available measurements, different approaches for fault estimation and accommodation have been proposed. In this area of research, there are many challenges such as decoupling the effect of concurrent faults, fault estimation in the presence of disturbances and modeling uncertainties, fault estimation accuracy and its effect on the fault accommodation process, etc.

1.1 Fault Estimation and Accommodation

A fault can be defined generally as any unexpected deviation of the system from the normal condition which can take place in the actuator, sensor or other components of the system [1]. Faults can deteriorate the system performance and may even lead to failure. Therefore, fault estimation and Fault-Tolerant Control (FTC) strategies become more critical in control design of a system in order to prevent instability or enhance the performance of the system. FTC strategies not only prevent catastrophic failure cases but reduces the maintenance cost and improve the safety and stability. Towards this end, faults need to be detected, isolated and estimated, the result of which can be used in the fault accommodation control methodology. Figure 1.1 illustrates the block diagram of a FTC scheme. As shown in this figure, faults can occur in the actuator, sensor or even in the components of the system. Hence, a methodology is required such that the affected faults can be estimated online. Once the fault is estimated, first this estimation can serve as a residual. Therefore by defining a proper threshold and decision making algorithm, fault detection and isolation is also possible. Then, the estimated value of fault can be used in order to redefine or modify the control strategy.

Fault estimation approaches can be categorized into two main classes: Data-driven and model-based approaches. Data-driven methodologies require significant quantities of data in healthy and faulty conditions of the system, while the model-based approaches require analytical and mathematical model of the system.

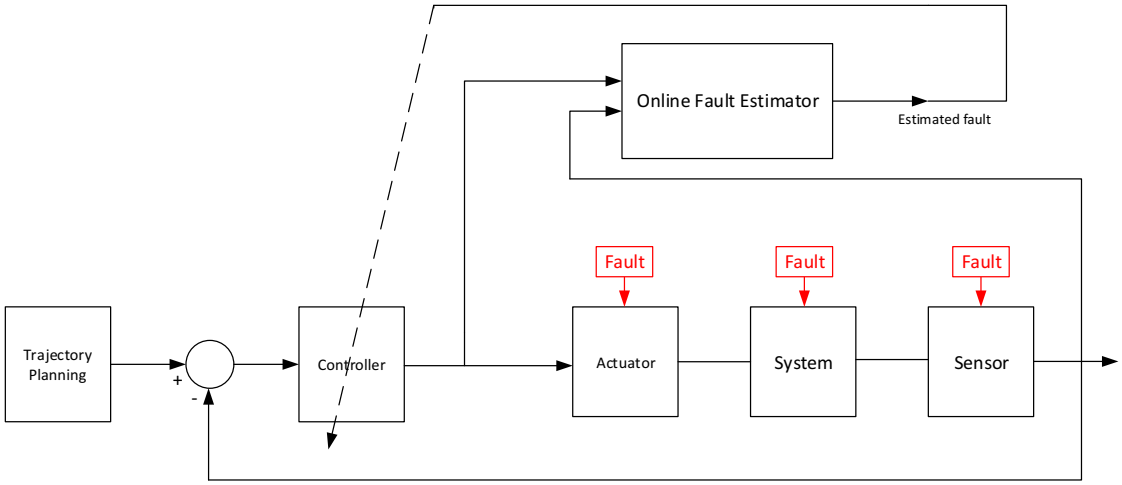

Figure 1.1: A general fault accommodation scheme

Moreover, the system can be affected by faults in different parts. From this point of view, faults can be classified into three types:

- Sensor faults
- Actuator faults
- Component faults

The main simplifying assumption considered in the literature to treat the faults is that only one type of fault affects the system. However, in more realistic scenario, different types of fault can occur in the system, simultaneously.

Further, in many fault estimation approaches, linear model of the system has been considered. In this case, though less complexity encountered, validity of the model is

decreased as we further deviate from the operating point. Moreover, considering the fact that any type of fault causes deviation from the operating point, we can conclude that linear approaches are not accurate and effective enough to deal with relatively large and significant faults.

As illustrated in Figure 1.1, the next step would be designing a FTC strategy using the estimated fault. Hence, the FTC schemes, proposed to minimize the performance degradation and avoid any dangerous situations, can be categorized into active and passive approaches. In passive FTC approaches, the controller is designed such that the robustness against the faults and unexpected deviations is guaranteed. However, in the active schemes, the controller will be reconfigured in the presence of faults such that the effect of fault is rectified.

The main challenge in developing both types of FTC scheme for nonlinear systems is modeling uncertainties. The control strategy should be designed such that the stability of the system is preserved in the presence of uncertainties, disturbances and measurement noises, as well as on the event of faults occurrence.

1.2 Motivation

Given the necessity of fault detection and estimation and consequently FTC strategy, different methodologies have been investigated in the literature, many of which have focused on one type of faults only. However, in many cases different types of faults can

take place simultaneously. In this work, the problem of concurrent sensor and actuator faults for a dynamical system modeled by Euler-Lagrange equations is investigated.

It should be noted that, a large class of physical system can be modeled by Euler-Lagrange (EL) equations. For instance, robot manipulators, industrial plants, autonomous vehicles can be modeled by EL equations. In this research, an Autonomous Underwater Vehicle (AUV) is considered as the case study and simulation results are provided for a 3 DOF AUV.

Moreover, considering modeling uncertainties, environmental disturbances and measurement noises, in this work a robust control approach is developed such that the faults can be detected, isolated and estimated, whilst the stability of the closed-loop system is also guaranteed. Furthermore, among the robust control approaches proposed in the literature, sliding mode methodology is used in this study. The reason for this choice is the interesting finite-time convergence properties of the sliding mode techniques.

1.3 Literature Review

As mentioned before, the first step for any FTC scheme is fault detection, isolation and estimation (FDIE). Thereupon, once the estimation of fault is obtained, it can be used in the underlying FTC. In the following section, a brief literature review on different developed FDIE approaches is provided.

1.3.1 Fault Detection, Isolation and Estimation

When a fault occurs in a system, it is necessary to first diagnose that the system is not working in its normal condition (Fault Detection). Thereupon, the next step is to determine the location of the fault (Fault Isolation). However, fault detection and isolation (FDI) cannot provide comprehensive information about the fault, such as the magnitude and nature of the fault. This information can be obtained by fault estimation process. Fault estimation is actually an extension for FDI, since an accurate estimation of the fault can be served as a residual which shows the occurrence and location of it.

General FDIE approaches use hardware and/or analytical redundancy. Hardware-redundancy or physical-redundancy is mostly applied in the aerospace and other critical systems. In this approach, multiple sensors, actuators or system components are augmented such that in the event of fault or failure, the normal operation is preserved. However, inclusion of extra sensor/actuator increases the cost and overall size. On the other hand, analytical-redundancy uses some kind of information in terms of nominal system behavior, either as a set of I/O data or physical model. The existing analytical-redundancy based FDIE approaches can be divided into data-based and model-based FDIE methodologies.

1.3.1.1 Data-Driven Methods

Data-driven or knowledge-based methods employ extensive measurement data in both healthy and faulty operations. For instance, in [2] and [3], a FDI methodologies based on human expert knowledge have been developed. Fuzzy-logic can also be employed to this end as explained in [4] and [5]. In some researches, neural networks used I/O data to fit a mathematical model or to detect and estimate the fault magnitude (see e.g. [6] and [7]).

The advantage of the data-driven methods is that in this approach, the explicit analytical model of the system is not required. Consequently, there would be relatively less mathematical complexity in applying this methodology. However in this case, a priori knowledge of extensive data for healthy situation and also for different faulty scenario is required. Moreover, well-established mathematical analysis and stability proof of the overall system require the application of analytical model-based approaches.

1.3.1.2 Model-Based Methods

Model-based or analytical redundancy approach is used to predict the healthy behaviour of the nominal system. The difference between the predicted value and the output measurement is defined as the residual. Hence, it can be concluded that while the residual is zero, there would be no fault in the system. However, any non zero value for

the residual indicates the occurrence of a fault in the system. Therefore, in the model-based approaches, the challenges are the residual generation and then a decision making algorithm for residual analysis. The residual generation techniques can be categorized into three main approaches [1]:

1. **Parity equations** [8, 9]: In this method, the so-called parity functions are used to extract the fault information by comparing the predicted and measured Input/Output of the system.

2. **Parameter estimation** [10, 11]: In this approach, some critical parameters of the system (such as the mass matrix in robotic systems) are estimated using online parameter-estimation methods. Thereupon, assuming the fault can change the parameters of the nominal system, the difference between the estimated and predetermined parameters can indicate the fault occurrence. Note that in this method, a priori knowledge of the system parameter is required. Therefore, considering the modeling error and uncertainties, a proper threshold is required in the residual analysis.

3. **State estimation** [12–18]: In this approach, an observer should be designed such that the outputs of the system are estimated from the I/O measurement. Thereafter, the difference between the estimated and measured output expresses the residual in this case. For residual analysis of the observer-based approaches, a

proper threshold is also required. Hence, once the residual exceeds the threshold, it can be interpreted as a fault occurrence in the system.

In most control applications, the persistency excitation condition, which is required for validity of parameter estimation approaches, is not met. Therefore, the accuracy of the performance of this method is questionable, while for the observer-based approaches, persistency excitation is not required. Basically, for observer-based approaches only the on-line measurement is required. Hence, in this work, an observer-based methodology is used to detect and estimate the faults.

The main observer-based FDIE approaches are investigated below:

1. **Unknown Input Observers (UIO)**: Based on the definition declared in [14], the UIO is an observer, the estimation error of which converges to zero despite of the presence of the unknown inputs. In the FDIE problem, it should be considered that in a realistic scenario, a system is always affected by disturbances and uncertainties. Hence, decoupling the effect of the disturbances and fault is an important issue in all related researches. Therefore, considering disturbances as an unknown input, UIOs are good candidates for solving this problem. The necessary and sufficient condition for the existence of an UIO is investigated by Kudva *et. al.* in [19]. This methodology is applied for linear systems in many researches e.g. [13]. Moreover, this approach is widely used in FDI for nonlinear systems. For example, in [20], an UIO is designed for a bilinear system such that the faults and failures occur

in actuators or sensors are detected and isolated. The authors in [21] presented a full-order UIO for Lipschitz nonlinear systems and also investigated the sufficient UIO existence condition with Linear Matrix Inequalities (LMI). Moreover, in [22] an UIO is used to detect, isolate and estimate simultaneous sensor and actuator faults affecting Lipschitz nonlinear systems. Seliger *et. al.* in [23] employed an UIO in conjunction with a robust methodology for nonlinear systems. Further, composite methodologies have also been proposed which consist of e.g. unknown input and a H_∞ observers in [24] and an unknown input and discrete-time sliding mode observers in [25]. In addition, the technique for solving FDI problem in [26] is composed of UIO and adaptive approaches. It is well-known that the reduced order observers have many advantageous over full-order observers. For instance, reduced order UIO is employed in [27] and [28].

2. **Adaptive Observers (AO)**: Adaptive techniques have shown promising results facing unknown/uncertain parameter cases. The principle of fault diagnosis using adaptive observers for linear systems was presented in [29]. In [30], an adaptive observer technique has been presented for FDI problem which also investigated the robustness against uncertainties. Another adaptive approach for fault diagnosis problem for nonlinear system in the presence of uncertainties or disturbances has been investigated in [31], in which geometric techniques are used for disturbance decoupling. In [32], an AO methodology in conjunction with a high gain observer

was proposed for nonlinear systems with unknown parameters and uncertainties in modeling. Adaptive sliding mode observer is used in [33] for fault diagnosis of an industrial gas turbine. Various adaptive techniques have also been used for fault diagnosis and fault-tolerant control in [34] and references therein.

Neural networks are popular in control and estimation applications due to their function approximation capabilities and the adaptive nature. For instance, a model-based adaptive nonlinear parameter estimation technique has been used in [35] to detect and isolate concurrent actuator fault of a reaction wheel actuator of the satellite attitude control system. Actuator fault detection and estimation for an industrial robotic arm was investigated extensively in [36] using a neural network observer. In [37], a robust neural-network-based actuator fault estimation is proposed for a nonlinear multi-tank system. Using this approach the influence of exogenous external disturbances was minimized. The authors in [6] proposed a recurrent neural network to solve sensor and actuator FDIE problem for general nonlinear system. However, the proposed scheme is inefficient for the case of having simultaneous sensor and actuator faults.

3. **Geometric approach**: Another commonly used FDIE technique for nonlinear systems is the so-called geometric approach. Geometric approach is a model-based

approach that solve the FDI problem based on some necessary and sufficient condition obtained from nonlinear system theories such as invariant subspace. Geometric approach is based on the pioneer work of [38] developed for linear systems. The extension of this work for nonlinear systems was presented in [39] by De Persis *et. al.*. In [40], sensor fault detection and isolation problem for nonlinear systems has been investigated using geometric tools. Dealing with time-delay systems, a geometric approach is used in [41]. The authors in [42] has employed geometric technique to solve the FDI problem for multi-dimensional systems. Moreover, a combination of neural network technique and geometric tools has been proposed for a satellite sensor and actuator fault in [43].

4. **Sliding Mode observers (SMO)**: Sliding mode technique was first introduced by Utkin in 1978 [44]. The principle of the observer using the sliding mode methodology was presented in [45]. Sliding mode observers have a great advantage over other nonlinear observers lend to the robustness properties of the sliding mode technique. Therefore, the stability of SMO is preserved even in the presence of disturbances, uncertainties and noises. Moreover, the most attractive feature of sliding mode technique is the finite-time convergence property. Having this property greatly simplifies the stability analysis of the overall closed-loop system. A composite algorithm consisting SMO and UIO was introduced in [46, 47]. Sliding

mode observers can also be used for solving FDI problem. Thereupon, if the dynamics of the system are known and no disturbance or noises affects the system, any deviation of the sliding term from zero can constitute the residual signal for FDI purposes. Further, in the presence of uncertainties in the model, disturbances and noises, the sliding term can be compared to a properly defined threshold. The fault reconstruction using SMO was introduced in the premium work of Edwards *et. al.* [18]. This work was extended in [48] by designing the sliding motion using H_∞ techniques such that the effects of uncertainties and disturbances are minimized. In this study, both sensor and actuator faults can be reconstructed using SMOs, however the scenario of having more than one type of faults was not considered. The survey paper [49] has provided a thorough review on both linear and nonlinear SMOs for FDI and fault reconstruction with required assumptions and necessary and sufficient conditions for stability analysis. In this review, it is shown that for sensor fault reconstruction, the so-called matching condition is required as well. In [50], a second order sliding mode observer was designed for FDI of a nonlinear system followed by a fault estimation algorithm. The problem of FDIE has been investigated in [51–53] for estimation of actuator faults for Lipschitz nonlinear systems. In [51], uncertainties with nonlinear bounds were considered in modeling and therefore a geometric coordinate transformation was used to eliminate the effects of uncertainties on the fault estimation. Some mechanical systems

are modeled with nonlinear equations with relative degrees from the inputs to the outputs higher than one. The problem of actuator fault detection, isolation and estimation of such systems has been considered in [52] under Lipschitz assumption by employing higher order SMOs. Considering the effect of uncertainties and disturbances, in [53] the authors presented a SMO for actuator FDIE in a nonlinear Lipschitz system. However, such imperfections were treated as input faults with a nonlinear distribution matrix. Sensor fault reconstruction for uncertain nonlinear systems was also investigated in [54]. In this work, a linear transformation was used to decouple the effects of disturbances.

Simultaneous Sensor and Actuator Faults: In most of the aforementioned work, only one type of faults i.e. either sensor or actuator faults has been considered. However, in a more realistic scenario, the system can be affected by simultaneous sensor and actuator faults. To detect, isolate and estimate simultaneous sensor and actuator faults, different approaches have been proposed in the literature. One approach is to use a bank of observers. In this technique, we need to have as many observers as the number of faults, each of which can detect and isolate one fault only. One way to tackle such problem is to design each observer such that it is sensitive to one fault only and therefore creates the nonzero residual in the presence of that specific fault. Whereas, in other approach, the observers are designed such that each observer is desensitized to one fault only. In this case, the decision making algorithm can detect and isolate a fault when

all the residuals are nonzero except one. As an example, a bank of high-gain observers is designed in [55] for fault detection and isolation in a nonlinear model of a chemical reactor system. The authors in [56] used a bank of observers to detect and isolate abrupt and incipient faults in nonlinear systems. In the residual analysis and decision making algorithm of this work, instead of a fixed threshold for all residuals, an adaptive approach is used for defining each threshold. However, by increasing the number of the states and actuators in a system, this approach is inefficient, since the number of the required observers increases dramatically. Hence, another approach to solve this problem is to consider faults as parameters of the system and subsequently employ adaptive observers. For instance, the authors in [57] investigated the simultaneous sensor and actuator FDIE for LTI systems affected by constant faults. However, persistently excitation condition is essential for accurate parameter estimation using adaptive techniques. The problem of simultaneous sensor and actuator faults can also be solved by robust techniques. Tan *et. al.* in [58] tackled this problem by using sliding mode observers for linear systems. In this work, by employing output transformation, proper filters and forming an augmented system, fault reconstruction has become possible. Raoufi *et. al.* in [59] presented a FDIE approach for Lipschitz nonlinear systems using SMOs in which simultaneous sensor and actuator faults have been considered. A novel linear transformation has been introduced such that the system is divided into two subsystems, one of which is affected by actuator fault and the other one is affected by sensor fault only. Thereupon, proper linear SMOs

were designed in this work such that the faults can be reconstructed and estimated. The same transformation has been used in [60] for Lipschitz nonlinear systems as well. However, in this work in order to relax the required matching condition for SMOs, an adaptive observer was designed instead. In most of the previous work, the nonlinear systems were studied under the Lipschitz assumption. However in general, physical systems can be modeled by different nonlinear functions which may not satisfy the Lipschitz condition.

Euler-Lagrange Systems: A large class of physical systems includes dynamical systems, the equations of motion of which are governed by Euler-Lagrange (EL) equations. Industrial robots, aerial vehicles and under water vehicles are a few to name as examples of EL systems. It is essential to develop reliable FDIE strategies for such systems. The problem of detection and isolation of the actuator faults was investigated in [61] for robot manipulator and [62] for an Unmanned Aerial Vehicles (UAV), using nonlinear observers. Moreover, sensor FDI problem for robot manipulators was solved using a bank of observers in [63]. Furthermore, for simultaneous sensor and actuator faults, FDI methodologies for a robotic arm were proposed in [64] using robust techniques and in [65] using data-driven approaches. In all aforementioned work, the fault estimation problem has not been tackled. In [66], one sensor or actuator fault have been considered for a robotic arm. However, it was assumed that the faults are not occur simultaneously. In

this work, the nonlinear model is considered to be Lipschitz and a SMO is used to estimate the faults. The problem of multiple actuator fault estimation for satellite systems have been addressed in [11, 62, 67] using adaptive observers and parameter estimation techniques such as least-square algorithm. Talebi *et. al.* considered the problem of multiple fault detection, isolation and estimation in either actuators or sensors using neural network based nonlinear observers [6]. Simultaneous fault detection and estimation in actuators and sensors have been considered in [68] using adaptive techniques. However, it was assumed that the faults can be expanded using some **known** basis functions, the assumption that limits the applicability of the approach.

1.3.2 Fault-Tolerant Control

On the event of fault occurrence, one concern is to detect, isolate and estimate the severity of the fault. However, the other concern targets the nominal performance of close-loop system. In fact, the original performance has to be preserved in the presence of faults (passive fault-tolerant control) or it has to be reconstructed once the system is subjected to any type of faults (active fault-tolerant control).

1.3.2.1 Active Fault-Tolerant Control

Most of the active fault-tolerant control schemes are based on rearranging the control structure/paramete according to the fault estimation properties. In [69, 70], a FTC

scheme was developed based on control allocation technique in which a virtual control input is first designed using sliding mode control. Then, a control allocation strategy is presented to distribute the control signal among the actuators such that the control action provided by faulty actuators are minimized based on weighted least square algorithm. For a planetary exploration vehicle modeled by Euler-Lagrange, an adaptive fault-tolerant control algorithm is designed in [71] such that the stability is guaranteed despite of the environmental disturbances. Thereupon, assuming that estimation of the fault is available, an optimal discrete control allocation algorithm was proposed to minimize the impact of fault occurrence on trajectory tracking.

In [72], an output (position) feedback fault-tolerant control allocation for flexible spacecraft modeled by EL equations was presented. Under the assumption of thruster redundancy, a robust least-squares-based control allocation was proposed which provides the optimal control solution minimizing the fault residual vector. The condition for employing this approach is that either physical redundancy is available or system controllability remains intact on the event of actuator failures.

Another widely studied methodologies in active FTC is estimation and compensation approach. In this approach, first the fault should be estimated online using one of the aforementioned methodologies. Thereafter, the effect of faults can be compensated using the information obtained from FE. An estimation and compensation approach for linear systems affected by either sensor or actuator faults has been proposed in [73].

For an uncertain linear system affected by actuator fault only, a bank of UIOs for fault estimation and sliding mode controller for system stabilization have been designed in [74]. In this work, the results of FE were used to reconfigure the controller and adjust the weight of the sliding surface. In [75], for a class of nonlinear systems affected by bias fault with healthy measurement, two fault-tolerant controllers have been designed. The first controller was used to guarantee the stability of the system in the presence of faults. Then, using a bank of adaptive estimators, the faults can be detected and isolated. Thereupon, the second fault-tolerant control approach minimizes the effects of faults on the tracking error.

The fault-tolerant control scheme proposed in [76] is a state feedback controller for Lipschitz nonlinear systems subject to actuator faults. The controller uses the estimation of system states provided by a robust observer. The proposed observer can simultaneously estimate the states and the actuator faults in the system. In [77], the concept of using estimation of the states and faults in designing the state feedback control rectifying the effect of fault, has been used. The fault estimation is obtained by employing adaptive techniques.

For a quad-rotor modeled by EL equations subjected to actuator faults only, a combination of a H_∞ observer and an adaptive fault-tolerant controller was proposed in [78]. In this paper, the fault information obtained from FE scheme is used to reconfigure the controller in order to enhance the tracking performance. To address the problem

of simultaneous sensor and actuator faults for nonlinear systems, two Takagi-Sugeno (T-S) fuzzy observers have been proposed in [79] to estimate corresponding sensor and actuator faults. Then, one T-S fuzzy controller have been presented which uses the fault estimation information to improve the tracking performance.

Adaptive control is a well-known approach for dealing with any sort of changes in system parameter and/or ambient conditions. In this approach, the parameters of the controller are updated based on the changes in system performance, in a sense that any imperfection arises from parameter deviations, environmental conditions, external disturbances and/or component/actuator faults can be accounted for.

For instance, an adaptive fault-tolerant scheme for linear systems with norm bounded uncertainties has been presented in [80]. The actuator faults are modeled as linearly parameterized functions with unknown time varying actuator efficiency coefficients which cover stuck, outage and loss of effectiveness. The controller consists of a constant gain obtained from LMI technique plus an adaptive gain updated based on the fault efficiency factor. In [81], for a Lipschitz nonlinear system with parametric uncertainties subjected to linearly parameterized actuator failure, a robust backstepping-based adaptive controller has been proposed. The performance of the approach was evaluated on a nonlinear model of a hypersonic aircraft.

The authors in [82], presented a FTC scheme composed of fuzzy logic and adaptive backstepping techniques for the attitude control of spacecraft in the presence of actuator

faults. The attitude is kinematically represented by singularity free unit quaternions. Moreover, parameter uncertainties (in mass moment of inertia) and external disturbances were also considered. In [83], an adaptive neural network-based FTC was designed for unknown Lipschitz nonlinear systems with multiple actuators subject to fault or failure.

An adaptive tracking control scheme for wheeled mobile robot with modeling uncertainties (uncertain/unknown center of mass) affected by actuator faults was addressed in [84]. In this work, the robot is modeled by EL equations and disturbances and uncertainties are assumed to be bounded. As mentioned before, adaptive techniques seem appropriate for FTC, since fault estimation is not required. However, adaptive approaches are developed based on the assumption of having fault free measurements [85]. Therefore, in the case of having sensor faults, adaptive approaches fail in providing a solution.

1.3.2.2 Passive Fault-Tolerant Control

The active FTC approaches studied so far relied on updating the control parameters/structure according to occurrence of faults. However, passive FTC approaches have fixed control structure and parameters. The controller is found such that the stability/performance of the closed-loop system is preserved even in the presence of faults. Hence, the robust control approaches are good candidates to tackle this problem. H_∞ optimal control yields promising results in robust stability and performance especially

for linear systems.

A robust H_∞ optimal controller was designed in [86] for uncertain linear system subjected to bounded uncertainties and sensor faults such that nominal performance is maintained in normal condition as well as in the event of sensor failures. The authors in [87] introduced a state feedback H_∞ controller for a discrete-time linear system subject to actuator faults and disturbances which enter into the system equations as piecewise affine functions. In [88] a robust fault-tolerant H_∞ control was given for an uncertain linear system affected by actuator and/or sensor failures. Robust fault-tolerant control schemes can also be employed for nonlinear systems. For example, in [89] this approach has been applied for attitude control of a flexible spacecraft in the presence of bounded disturbance and loss of effectiveness actuator fault.

A simultaneous fault detection and control problem for switched linear systems has been addressed in [90] . The H_∞ and H_- criteria have been used to optimize the control and fault detection problem. The optimization problem is cast in such a way that the effects of disturbances and faults on control objective are minimized whereas the effect of faults on residual is maximized.

Another popular robust FTC technique for dealing with different types of fault in a system employed widely in the literature is Sliding Mode Control (SMC) approach. In this technique, for compensating the effect of uncertainties, disturbances and faults, a discontinuous sliding term is added to the controller. This sliding term is a function of

tracking error and force the system to slide along a desired cross-section of its nominal behavior.

A full-rank SMC was introduced in [91] for uncertain linear system subject to uncertainties and quantization. The proposed controller guaranteed the closed-loop system asymptotic stability even in the presence of actuator faults. The authors in [92] introduced a robust SMC scheme for attitude control of a satellite which is modeled by EL equations. The stability of the closed-loop system was ensured by the designed controller, in the presence of actuator loss of effectiveness and external disturbances.

In [93], a sliding mode controller was presented for a 6 DOF vehicle suspension system affected by additive actuator faults only. However, the presented model was a linear. Hence in this work, the controller should preserve the stability not only against uncertainty, disturbances and faults, but also in the presence of neglected nonlinearities.

The authors in [94] have presented a new higher order SMC in which the estimation of the fault is required to update the sliding surface through an adaptive technique. It is claimed that using this adaptive SMC approach, better transient and faster convergence can be obtained. This method has been evaluated on a robot manipulator modeled by EL equations subject to actuator faults only.

It is worth mentioning that, similar fault reconstruction methodology to that of SMO can be used for SMC as well.For example in [95], first a SMC was designed to stabilize a second order uncertain system subject to disturbances. Thereafter, from

analysing the sliding term of the controller, the disturbances have been reconstructed. The authors in [96] proposed a SMC for a DC motor subject to unmatched uncertainties and disturbances such that not only the stability of the closed-loop system is guaranteed but also the disturbances and uncertainties can be reconstructed. Therefore, considering the fault as a kind of system uncertainty, it can be reconstructed and estimated from analysing the sliding surface as well.

Most of the aforementioned work on FDIE and FTC have focused on one type of faults only, i.e. either an actuator or sensor faults. A few work which developed FDIE strategies for simultaneous actuator and sensor faults suffer from some constraining assumptions such as Lipschitz nonlinearities, requirement for rich (persistently) excitation and/or knowing the basis functions of the fault signal. Some other work has also been developed for specific physical systems such as robot manipulators or satellite systems. The primary aim of this research is to develop fault accommodation strategies which treat general Euler-Lagrange systems affected by simultaneous sensor and actuator faults with no limiting assumption mentioned above. Toward this end, two different approaches will be introduced.

1. The first fault accommodation strategy proposed in this research is an active fault-tolerant control. In this regard, a novel FDIE methodology will be presented. Two sliding mode observers are employed to reconstruct corresponding sensor and actuator faults. Thereafter, the estimated values of faults are used to reconfigure

the control action.

2. In second proposed fault-tolerant control scheme, only the sensor fault estimation is used. However, to compensate the effects of actuator faults, a robust sliding mode control methodology is employed.

1.4 Euler-Lagrange Modeling Approach

In this section, the general procedure for driving equations of motion using EL approach is given. Systems modeled by EL formulations possess some interesting properties which help us in analysing the FDIE and FTC methods developed in later chapters. Some of these properties are given in this section. Finally, the equations of motion of an AUV considering environmental disturbances is provided.

The Euler-Lagrange differential equation is the fundamental equation of calculus of variations which states that if $\mathcal{S}$ is defined by an integral below:

$$\mathcal{S} = \int_{t_1}^{t_2} f(t, x, \dot{x}) dt \tag{1.1}$$

Then $\mathcal{S}$ has a minimum value if the following Euler-Lagrange differential equation is satisfied.

$$\frac{\partial f}{\partial x} - \frac{d}{dt}(\frac{\partial f}{\partial \dot{x}}) = 0 \tag{1.2}$$

The principle of least action states that the if the action $\mathcal{S}$ above is defined by the integral of the kinetic energy minus potential energy, then it has its minimum value

for the actual system motion. Hence, the system equation of motion can be obtained by the Euler-Lagrange differential equation. The heart of EL approach is the so-called Lagrangian defined by:

$$\mathcal{L} \quad = \quad \mathcal{K}(q, \dot{q}) - \mathcal{P}(q) \tag{1.3}$$

where q is the generalized coordinate of the system, $\mathcal{K}$ is the kinetic energy which depends on generalized coordinates of the system and their derivatives and $\mathcal{P}$ is the potential energy which is a function of generalized coordinates only. Hence, the first step to obtain the dynamic model is to define the generalize coordinate and then find the kinetic and potential energies in terms of the generalize coordinates and their derivatives. Then, the Lagrangian formulation is given by:

$$\frac{d}{dt}\frac{\partial \mathcal{L}}{\partial \dot{q}_i} - \frac{\partial \mathcal{L}}{\partial q_i} \quad = \quad \tau_i \tag{1.4}$$

where τ_i is the generalized force acting on the i^{th} generalized coordinate which includes external as well as the constrained forces. The EL equation is generally shown in the following compact form:

$$M(q)\ddot{q} + C_{co}(q, \dot{q})\dot{q} + G(q) \quad = \quad \tau \tag{1.5}$$

where τ denotes the input torque (force), $M(q)$ represents the inertia matrix, $C_{co}(q, \dot{q})$ is the matrix of Coriolis and centripetal terms, and $G(q)$ shows the gravity vector.

The following properties are hold for systems modeled by (1.5) [97]:

Property 1. *The inertia matrix for a rigid robot is symmetric and positive definite.*

Property 2. *The inertia matrix is bounded by functions of the position of the joints. However, if all joints are revolute then the inertia matrix contains only bounded functions of the joint variables, that is, terms containing trigonometric functions and therefore the inertia matrix as well as its inverse are bounded .*

Property 3. *For mechanical systems with rotary joints, the gravity vector consists of trigonometric functions of position and therefore is bounded as well.*

Furthermore it is worth mentioning that, based on [97], the elements of Coriolis matrix are obtained as follows:

$$C_{kj} = \sum_{i=1}^{n} \frac{1}{2}\{\frac{\partial M_{kj}}{\partial q_i} + \frac{\partial M_{ki}}{\partial q_j} - \frac{\partial M_{ij}}{\partial q_k}\}\dot{q}_i \tag{1.6}$$

where C_{kj} are the elements of C_{co}. The definition of Coriolis matrix shows that, the elements of $C_{co}(q, \dot{q})$ are trigonometric functions of position and quadratic terms of velocities such as $\dot{q}_i\dot{q}_j$ and $\dot{q}_i^2$.

1.4.1 Modeling of Autonomous Underwater Vehicles

The equations of motion of an autonomous underwater vehicle (AUV) can also be obtained by (1.5). As illustrated in Figure 1.2, the generalized coordinate q can be interpreted as the position of an AUV expressed in inertial or body-fixed frame. Inertial or

earth-fixed frame is a fixed reference coordinate frame while body-fixed frame is rigidly attached to the AUV.

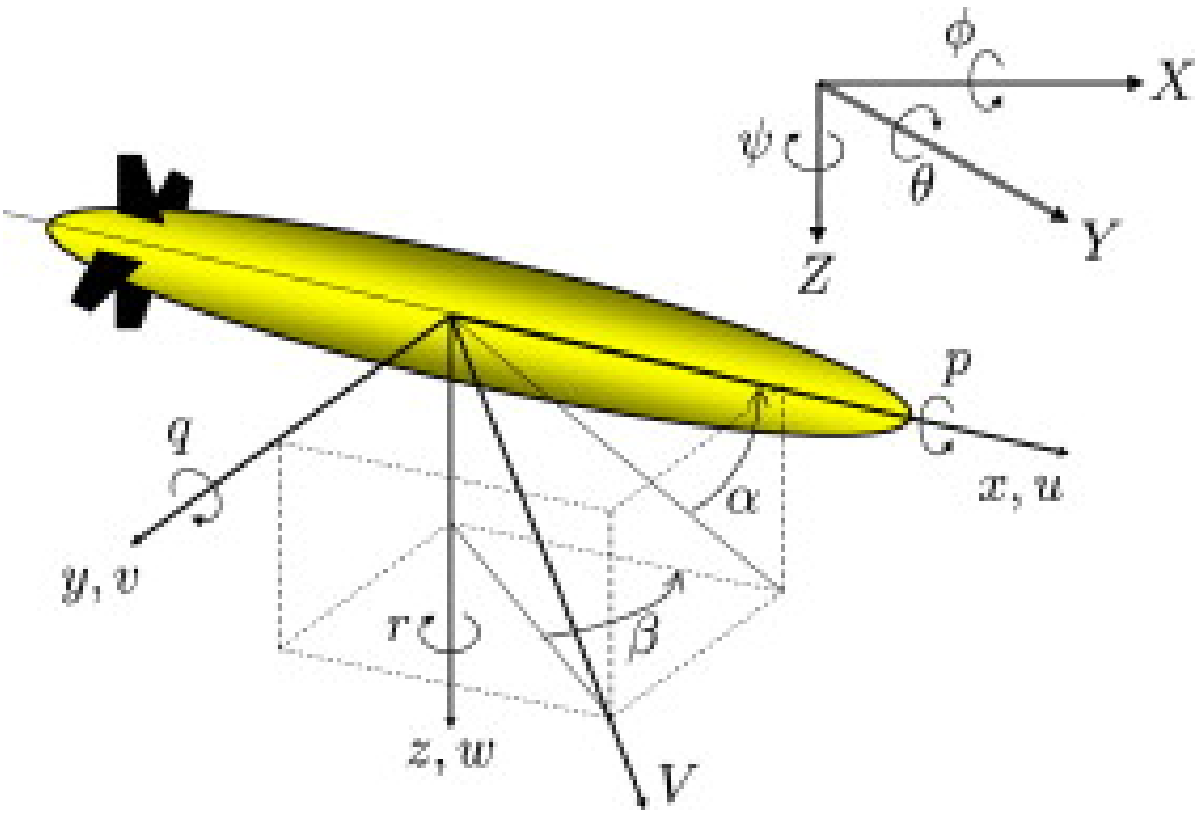

Figure 1.2: Expression of body-fixed and earth-fixed frames for an AUV [98]

Hence, according to Figure 1.2, for a 6 DOF AUV, $q = [X, Y, Z, \phi, \theta, \psi]^T$ where X, Y and Z show the position of the mass center of the AUV with respect to the origin of the inertial frame and ϕ, θ and ψ are the Euler angles denote the orientation of the AUV body-fixed frame. Moreover, by denoting $V = [u, v, w, p, q, r]^T$ as the linear and angular velocity vector of the AUV, we get:

$$\dot{q} \;=\; RV \tag{1.7}$$

where R can be found using the Euler angles in the following form:

$$R = \begin{bmatrix} R_1 & 0 \\ 0 & R_2 \end{bmatrix} \tag{1.8a}$$

$$R_1 = \begin{bmatrix} c\psi c\theta & -c\phi s\psi + s\phi s\theta c\psi & s\phi s\psi + c\phi s\theta c\psi \\ c\theta s\psi & c\psi c\phi + c\psi s\theta s\phi & -s\phi c\psi + c\phi s\theta s\psi \\ -s\theta & s\phi c\theta & c\phi c\theta \end{bmatrix} \tag{1.8b}$$

$$R_2 = \begin{bmatrix} 1 & s\phi t\theta & c\phi t\theta \\ 0 & c\phi & -s\phi \\ 0 & s\phi/c\theta & c\phi/c\theta \end{bmatrix} \tag{1.8c}$$

Once the position and velocity kinematics are done, the EL approach can be employed to obtain the dynamic equations in body-fixed frame as [99]:

$$M_V\dot{V} + C_{coV}(V)V + N_V V \;=\; \tau_V \tag{1.9}$$

where M and $C_{co}(V)$ are the inertia and Coriolis matrices given in (1.5), and N is the damping matrix .

If the motion of the AUV is limited in a plane, a reduce-order model, i.e. a 3

DOF equations of motion can be considered instead. Let us now define, $q = [x, y, \psi]$ and $V = [u, v, r]$, then the corresponding matrices are now given by:

$$M_V = \begin{bmatrix} m_{11} & 0 & 0 \\ 0 & m_{22} & m_{23} \\ 0 & m_{23} & m_{33} \end{bmatrix} \tag{1.10}$$

$$C_{coV} = \begin{bmatrix} 0 & 0 & -(m_{22}v + m_{23}r) \\ 0 & 0 & m_{11}u \\ m_{22}v + m_{23}r & -m_{11}u & 0 \end{bmatrix} \tag{1.11}$$

$$N_V = \begin{bmatrix} n_{11} & 0 & 0 \\ 0 & n_{22} & n_{23} \\ 0 & n_{23} & n_{33} \end{bmatrix} \tag{1.12}$$

where in M_V and $C_{co}(V)$, the effect of added mass is also considered. Thereafter, using the transformation matrix R in (1.8), we can express the dynamic equations in earth˙frame as follows:

$$M_o(q)\ddot{q} + C_{co}(q, \dot{q})\dot{q} + N_o(q)\dot{q} = \tau_l \tag{1.13}$$

where

$$M_o(q) = R^{-T}(q) M_V R^{-1} \tag{1.14}$$

$$C_{co}(q, \dot{q}) = R^{-T}(q)[C_{coV} - M_V R^{-1} \dot{R}] R^{-1} \tag{1.15}$$

$$N_o(q) = R^{-T} N_V R^{-1} \tag{1.16}$$

$$\tau_l = R^{-T} \tau_V \tag{1.17}$$

Moreover, the effects of environmental disturbances such as ocean current and modeling uncertainties can be considered as an additive term to dynamic equations in the form of:

$$M_o(q)\ddot{q} + C_{co}(q, \dot{q})\dot{q} + N_o(q)\dot{q} = \tau_l + \Delta f \tag{1.18}$$

In [99], the ocean current is modeled as a drift.

$$\Delta f = J^{-1} d_c \tag{1.19}$$

where J is the proper Jacobian matrix and $d_c = [d_{cx} \quad d_{cy} \quad 0]^T$ is a constant or slowly varying bias:

$$\dot{d}_c = w_d \tag{1.20}$$

where w_d is a vector of zero mean Gaussian white noise process.

1.4.2 Actuator Dynamics

In this section, the actuator (DC motor) dynamics will be presented. A DC motor can be modeled by a second order system as follows [97]:

$$J_m\ddot{q} + B\dot{q} \;=\; \tau - \tau_l \tag{1.21}$$

where J_m is a diagonal matrix representing the inertia of the motors and B is a diagonal matrix corresponding to the damping of the motors shafts. Moreover, τ denotes the motor torque and τ_l shows the loading torque related to the AUV rigid body dynamics (1.18). Hence, by substituting (1.18) into (1.21), one can obtain:

$$M(q)\ddot{q} + C_{co}(q,\dot{q})\dot{q} + N(q)\dot{q} \;=\; \tau + \Delta f \tag{1.22}$$

where $M(q) = M_o(q) + J_m$ and $N(q) = N_o + B$. Note that, similar properties hold for the augmented inertia matrix $M(q)$. Moreover, the Coriolis and centrifugal terms remains unchanged in (1.22).

1.5 Problem Statement

Consider the following nonlinear system governed by the Euler-Lagrange equations:

$$M(q)\ddot{q} + C_{co}(q,\dot{q})\dot{q} + G(q) \;=\; \tau \tag{1.23}$$

where q is the generalized coordinate, τ denotes the input torque (force), $M(q)$ represents the inertia matrix, $C_{co}(q,\dot{q})$ is the matrix of Coriolis and centripetal forces, and $G(q)$

denotes the gravity vector.

The state space representation of the above system can be expressed as follows:

$$\begin{aligned} \dot{x}_1 &= x_2 \\ \dot{x}_2 &= M^{-1}(x_1)(\tau - C_{co}(x_1, x_2)x_2 - G(x_1)) + \Delta f \end{aligned} \tag{1.24}$$

where $x = [x_1^T \quad x_2^T]^T \in \mathbb{R}^n$ denotes the state vector of the system, $x_1 = q$ is the position vector and $x_2 = \dot{q}$ denotes the velocity vector. Moreover in (1.24), Δf represents the uncertainties, unmodeled dynamics and disturbances in the system. Therefore, the system with both actuator and sensor faults can be expressed as follows:

$$\begin{bmatrix} \dot{x_1} \\ \dot{x_2} \end{bmatrix} = \begin{bmatrix} x_2 \\ f(x) + \Delta f \end{bmatrix} + \begin{bmatrix} 0 \\ g(x) \end{bmatrix} (\tau + f_a) \tag{1.25}$$

$$y = Cx + D_s f_s \tag{1.26}$$

where $y \in \mathbb{R}^n$ denotes the output vector, $f_a \in \mathbb{R}^m$ and $f_s \in \mathbb{R}^q$ denote unknown bounded actuator and sensor faults, respectively. Moreover in (1.25), $f(x) = M^{-1}(x_1)(-C_{co}(x_1, x_2)x_2 - G(x_1))$ and $g(x) = M^{-1}(x_1)$.

The objective of this thesis is to develop fault estimation, accommodation, and control strategies for nonlinear system (1.25)-(1.26) under Assumptions 1 and 2 such that:

- The FTC approaches should preserve the closed-loop system stability in the presence of uncertainties, disturbances and simultaneous sensor and actuator faults.

- It is desired that the FTC approaches result in a small tracking error in the presence of faults, uncertainties and disturbances, i.e. $\lim_{t\to\infty} y(t) \approx y_d(t)$, where $y_d(t)$ is a smooth desired trajectory.

- It is further desired that for the FDIE approaches, the fault estimation errors converge to zero asymptotically, i.e. $\lim_{t\to\infty} \hat{f}_a = f_a$ and $\lim_{t\to\infty} \hat{f}_s = f_s$, where $\hat{f}_a$ and $\hat{f}_s$ are the estimations of actuator and sensor faults, respectively.

  Towards these objectives, the following assumptions are made:

Assumption 1. *The sensor fault distribution matrix $D_s \in \mathbb{R}^{n\times q}$ has full column rank.*

Assumption 2. *The sensor and actuator faults, the uncertainties, unmodeled dynamics, and disturbances are unknown but are bounded and the bounds are known, that is $\|f_s\| < \bar{f}_s$, $\|f_a\| < \bar{f}_a$ and $\|\Delta f\| < \Delta\bar{f}$ for all t.*

1.6 Thesis Contributions

The contribution of this thesis is threefold.

- First, we develop a robust FDIE strategy for EL nonlinear systems subject to simultaneous actuator and sensor faults without Lipschitz or other limiting conditions stated in Literature Review. The linear coordinate transformation and output redefinition introduced in [59] will be extended to this class of nonlinear

systems. The linear transformation, which does not depend on the nonlinearities of the system, decouple the system dynamics into two subsystems, each of which is affected by one type of fault only. Next, the sensor and actuator faults can be estimated using separate SMOs. It is worth mentioning that the extension is made in a sense that the system considered in this research is a general affine nonlinear model unlike [59] which considers an additive Lipschitz nonlinear term and linear input matrix. Furthermore, no specific algorithm has been presented in the literature to find the output transformation. In this thesis, a systematic approach based on Linear Matrix Inequalities (LMI) is presented to obtain the transformation.

- An active fault-tolerant control strategy is provided which uses the results of sensor and actuator fault estimations to reconfigure the controller. The mathematical proof of stability is provided for the overall system consisting of two observers, the actual system and the reconfigured controller. Note that the challenges arise from the fact that the observers, the nonlinear system and the controller are tightly coupled. The finite time convergence properties of sliding mode observers and the properties of Euler-Lagrange systems will be used in the stability analysis.

- Another fault-tolerant control scheme introduced in this work uses the same transformations to decouple the effects of sensor and actuator faults. However, only one SMO is employed to estimate the sensor faults, the result of which will be used in control reconfiguration. The actuator fault, on the other hand is accounted for

via a robust sliding mode control approach. In this way, the robustness against actuator faults as well as fault reconstruction is guaranteed. Stability analysis of the closed-loop system including the nonlinear system, the coupled sliding mode observer and controller is also demonstrated.

1.7 Thesis Outline

This dissertation is given in 5 chapters, the outline of which is presented below.

Chapter 1: Introduction In this chapter, first a brief introduction to fault estimation and accommodation problem has been given. Next, the motivation of this research was provided and the available FDIE and FTC strategies in the literature have been reviewed. Moreover, the principles of Euler-Lagrange modeling approach has been given. Thereupon, equations of motion for an Autonomous Underwater Vehicle (AUV) have been driven using EL methodology. Finally, the problem addressed in this thesis was stated and contributions have been highlighted.

Chapter 2: The Sensor and Actuator Fault Decoupling Strategy This chapter presents the required linear coordinate and output transformations to decompose the system into two subsystems. Subsystem 1 is affected by sensor faults only whereas Subsystem 2 is affected by actuator faults. Note that, no Lipschitz condition or a *priori* knowledge about the system nonlinearities are required to obtain these transformations.

Subsequently, an analytical approach is presented to find coordinate transformation using LMI. Finally, in order to reconstruct the sensor fault associated with Subsystem 1, a new set of exo-states is introduced such that the sensor faults enter the system equations as an unknown input.

Chapter 3: The Proposed Active Fault Accommodation Scheme Using Sliding Mode Observers Once the effects of sensor and actuator faults are separated, corresponding sensor and actuator fault estimation and reconstruction can be readily achieved by using two SMOs. The resulting fault estimations are used to reconfigure the controller. Finally, the mathematical proof of stability for the coupled controller, observers and nonlinear plant is demonstrated.

Chapter 4: The Proposed Active Fault-Tolerant Control Strategy Using Sliding Mode Controller and Observer Using the same decoupling methodology, a robust fault-tolerant control scheme is introduced based on sliding mode controller. In this approach, only the sensor fault estimation is fed back to the controller in order to correct the faulty measurement. However to deal with actuator faults, a robust sliding mode controller is used. As a result, the tracking performance is preserved in the presence of actuator faults. Moreover, the actuator fault reconstruction can also be performed by using the controller sliding surface.

Chapter 5: Conclusions and Future Work In this chapter concluding remarks about the thesis contributions and adopted methodologies are given. Moreover, suggestions for further research will be provided.

Chapter 2

The Sensor and Actuator Fault Decoupling Strategy

2.1 Introduction

In this chapter, linear coordinate and output transformations are introduced to decompose the underlying nonlinear system into two subsystems where the effects of the sensor and actuator faults are decoupled from each other. Towards this end, first the output redefinition matrix S is found using LMI and subsequently coordinate transformation T is obtained.

Consequently, in order to estimate the sensor fault, a set of exo-state needs to be augmented to the system such that the sensor faults appear as an unknown input

to the new system. Finally, to estimate the unknown input, a nonsingular coordinate transformation T_u is utilized. Using the augmented subsystem, not only estimation of the sensor fault is possible, but also accurate estimate of the states that becomes unavailable during the presence of faults, can also be obtained.

2.2 Coordinate and Output Transformations

Consider the nonlinear system given in (1.25)-(1.26) and repeated here:

$$\begin{bmatrix} \dot{x_1} \\ \dot{x_2} \end{bmatrix} = \begin{bmatrix} x_2 \\ f(x) + \Delta f \end{bmatrix} + \begin{bmatrix} 0 \\ g(x) \end{bmatrix} (\tau + f_a) \tag{2.1}$$

$$y = Cx + D_s f_s \tag{2.2}$$

where $x \in \mathbb{R}^n$ is the state vector of the system, $\tau \in \mathbb{R}^m$ is the control input, $y \in \mathbb{R}^n$ denotes the output vector. In other words, it is assumed that the full-sates measurement is available. Moreover, $f_a \in \mathbb{R}^m$ and $f_s \in \mathbb{R}^q$ denote unknown bounded actuator and sensor faults, respectively.

As mentioned in Section 2.1, an output re-definition transformation S and a state space coordinate transformation T are required to decouple the effect of sensor and actuator faults. Towards this end, it is required to transform the output matrix to a block diagonal form, which is implied that one set of output is fully desensitized to sensor fault and the other set is fully desensitized to the actuator fault. Hence, we define:

$$h = Tx, \quad w = Sy \tag{2.3}$$

such that the transformed system matrices become:

$$T \begin{bmatrix} 0 \\ g(x) \end{bmatrix} = \begin{bmatrix} 0 \\ g(T^{-1}h) \end{bmatrix}, \tag{2.4}$$

$$SCT^{-1} = \begin{bmatrix} C_1 & 0 \\ 0 & C_4 \end{bmatrix}, \qquad SD_s = \begin{bmatrix} D_{s1} \\ 0 \end{bmatrix}$$

where $T \in \mathbb{R}^{n\times n}$, $S \in \mathbb{R}^{n\times n}$, $C_1 \in \mathbb{R}^{(n-m)\times(n-m)}$, $C_4 \in \mathbb{R}^{m\times m}$, and $D_{s1} \in \mathbb{R}^{(n-m)\times q}$.

As for output redefinition, let us define the matrix S. In order to achieve the transformed system matrices as in (2.4), the matrix S should be defined such that:

$$SD_s = \begin{bmatrix} D_{s1} \\ 0 \end{bmatrix} \tag{2.5}$$

$$SC = \begin{bmatrix} C_1 & 0 \\ C_{S03} & C_4 \end{bmatrix} \tag{2.6}$$

where C_4 is a full rank matrix. In other words, the aim of introducing S is to partition D_s and C such that the last m states are completely decoupled from sensor faults. To find such transformation, the matrix S is factorized into two matrices $S_0 \in \mathbb{R}^{n\times n}$ and $S_1 \in \mathbb{R}^{n\times n}$ such that $S = S_1 S_0$. Then, the nonsingular transformation S_0 should be selected such that

$$S_0 D_s = \begin{bmatrix} D_{s1} \\ 0 \end{bmatrix} \tag{2.7}$$

where $D_{s1} \in \mathbb{R}^{(n-m)\times q}$ is a full column rank matrix as defined in (2.4). Moreover, the

selected S_0 should yield

$$S_0 C = \begin{bmatrix} C_{S01} & C_{S02} \\ C_{S03} & C_4 \end{bmatrix} := C_s \tag{2.8}$$

where $C_{S01} \in \mathbb{R}^{(n-m)\times(n-m)}$ and $C_4 \in \mathbb{R}^{m\times m}$. As the above equations show, the rational behind this factorization is to partition D_s and C via S_0 and S_1, respectively.

To find S_0, it is necessary to ensure that C_4 is nonsingular. On the other hand, the matrix S_1 should be obtained in such a way that it has no effect on the partitioning of $\begin{bmatrix} D_{s1} \\ 0 \end{bmatrix}$, whereas it transforms the output matrix C_s to a lower triangular matrix as given in (2.6). Consequently, one choice of S_1 can be given as:

$$S_1 = \begin{bmatrix} I_{n-m} & -C_{S02}C_4^{-1} \\ 0 & I_m \end{bmatrix} \tag{2.9}$$

Hence, by defining $S = S_1 S_0$ one can get (2.6), where $C_1 = C_{S01} - C_{S02}C_4^{-1}C_{S03}$. Moreover, the definition of S_1 as in (2.9) results in:

$$SD_s = S_1 S_0 D_s = \begin{bmatrix} I_{n-m} & -C_{S02}C_4^{-1} \\ 0 & I_m \end{bmatrix} \begin{bmatrix} D_{s1} \\ 0 \end{bmatrix} = \begin{bmatrix} D_{s1} \\ 0 \end{bmatrix} \tag{2.10}$$

Note that the function of the transformation S_0 is to shift the rows of the matrices C and D_s for decoupling purposes and it is straightforward to obtain it by using elementary matrix operations. However, since there is a restriction that the resulting matrix contains one full rank block (i.e. C_4), a matrix equality (inequality) solver, e.g. any LMI solver, can be used to solve for a proper S_0 that also satisfies C_4 rank condition. Towards this

end, the matrix S_0 needs to satisfy (2.7) where D_{s1} is full column rank. Moreover, in (2.8), there is no rank constraint on matrices C_{S01} , C_{S02} , and C_{S03}. In (2.7)-(2.8) we have two matrices S_0 and C_s that can be solved by a proper LMI solver. However, since the final value of the transformed matrices in (2.4), may affect other parts of our methodology, the LMI conditions will be represented later in this chapter.

As (2.4) shows, the transformed output matrix (SCT^{-1}) must be a block diagonal matrix. Moreover, the coordinate transformation matrix T transforms the input matrix as well. However, it is desirable that the partitioned form of the nonlinear input matrix $\begin{bmatrix} 0 \\ g(x) \end{bmatrix}$ is preserved, i.e.

$$T \begin{bmatrix} 0 \\ g(T^{-1}h) \end{bmatrix} = \begin{bmatrix} 0 \\ g(T^{-1}h) \end{bmatrix}$$

Consequently, given that C_4 is full-rank, the state transformation T may be selected as:

$$T = \begin{bmatrix} I_{n-m} & 0 \\ T_3 & I_m \end{bmatrix} \tag{2.11}$$

where $T_3 = C_4^{-1}C_{S03}$. Now, T^{-1} can be obtained as:

$$T^{-1} = \begin{bmatrix} I_{n-m} & 0 \\ -C_4^{-1}C_{S03} & I_m \end{bmatrix} \tag{2.12}$$

Then, it is straightforward to show that (2.4) is hold.

By substituting the transformation (2.11) into (2.3), one can get the following

expressions

$$h_1 = x_1, \quad h_2 = T_3 x_1 + x_2, \quad h = [h_1^T, h_2^T]^T$$

Therefore, using the above state transformation and output redefinition $w = Sy$, the overall transformed and decoupled system dynamics can be expressed as

$$\underline{\text{Subsystem 1:}}$$
$$\begin{cases} \dot{h}_1 = -T_3 h_1 + h_2, \\ w_1 = C_1 h_1 + D_{s1} f_s, \end{cases} \tag{2.13}$$
$$\underline{\text{Subsystem 2:}}$$
$$\begin{cases} \dot{h}_2 = \bar{f}(T^{-1}h) + \Delta f + g(T^{-1}h)(\tau + f_a), \\ w_2 = C_4 h_2, \end{cases} \tag{2.14}$$

where $w = [w_1^T \quad w_2^T]^T = Sy$ and $\bar{f}(T^{-1}h) = T_3 h_2 - T_3^2 h_1 + f(T^{-1}h)$.

The decoupled dynamic equations above can be used to design state observers for sensor and actuator faults reconstruction. However, for accurate state estimation, it is required that a subset of output be available which is not contaminated by faults and shows the actual values of system states. In (2.13) and (2.14), the output of Subsystem 2 is decoupled from sensor faults. Hence, the states of this subsystem as well as actuator faults can be accurately estimated using e.g. sliding mode observers.

However, note that the output of Subsystem 1 is contaminated by sensor faults. Therefore, it is necessary to define a set of exo-states such that the sensor faults enter in the state equations not as output faults but as unknown inputs. This allows us

to accurately estimate the states of Subsystem 1 and reconstruct sensor faults using a sliding mode observer.

Towards this end, an auxiliary state $z = \int_0^t w_1(\tau)d\tau$ is introduced. Therefore, the dynamics associated with this new state is governed by

$$\dot{z} \;\; = \;\; C_1 h_1 + D_{s1} f_s$$

The resulting new augmented system containing $2(n-m)$ states can now be defined as follows:

$$\underline{\text{Subsystem 1:}}$$

$$\begin{cases} \dot{h}_z = A_z h_z + \begin{bmatrix} I_m \\ 0 \end{bmatrix} h_2 + \begin{bmatrix} 0 \\ D_{s1} f_s \end{bmatrix}, \\ w_z = C_z h_z, \end{cases} \tag{2.15}$$

$$\underline{\text{Subsystem 2:}}$$

$$\begin{cases} \dot{h}_2 = \bar{f}(T^{-1}h) + \Delta f + g(T^{-1}h)(\tau + f_a), \\ w_2 = C_{S04} h_2, \end{cases} \tag{2.16}$$

where $h_z = \begin{bmatrix} h_1 \\ z \end{bmatrix}$, $A_z = \begin{bmatrix} -T_3 & 0 \\ C_1 & 0 \end{bmatrix}$, $C_z = [0 \quad I_{n-m}]$, and therefore $w_z = z$. In the above representation, the sensor fault f_s only affects Subsystem 1 in (2.15) and the actuator fault f_a only affects Subsystem 2 in (2.16).

It should be noted that, the accurate measurement of h_1 is not available at the instant that a sensor fault occurs. Therefore, h_1 state estimation error cannot be used

to form the sliding motion and guarantee the stability of the observer. Hence, a state transformation on h_1 is required, as a result of which a stable sliding motion can take place invariant of sensor faults. In other words, the transformation should guarantee the stability as well as decoupling the sliding motion from sensor faults. Towards this end the following state transformation matrix on h_z is proposed :

$$T_u = \begin{bmatrix} I_{n-m} & L_0 \\ 0 & I_{n-m} \end{bmatrix} \tag{2.17}$$

which leads to a new state vector $q := [q_1^T \quad q_2^T]^T = T_u h_z$, where $q_1, q_2 \in \mathbb{R}^{n-m}$. The transformed state equations can be expressed as:

$$\begin{aligned} \dot{q} &= A_q q + \begin{bmatrix} I_m \\ 0 \end{bmatrix} h_2 + \begin{bmatrix} L_0 D_{s1} f_s \\ D_{s1} f_s \end{bmatrix} \\ w_3 &= [0 \quad I_{n-m}] q \end{aligned} \tag{2.18}$$

where

$$\begin{aligned} A_q &= \begin{bmatrix} A_{q1} & A_{q2} \\ A_{q3} & A_{q4} \end{bmatrix} \\ &= \begin{bmatrix} -T_3 + L_0 C_1 & T_3 L_0 - L_0 C_1 L_0 \\ C_1 & -C_1 L_0 \end{bmatrix}. \end{aligned}$$

Based on our earlier discussion, the matrix gain L_0 should satisfy the following stability

and decoupling conditions:

$$(-T_3 + L_0C_1)^T P + P(-T_3 + L_0C_1) = -Q \tag{2.19}$$

$$L_0 D_{s1} = 0 \tag{2.20}$$

Note that, the second equation above represents the so-called matching condition. Next, by substituting (2.20) into (2.18), one can get:

$$\begin{aligned} \dot{q} &= A_q q + \begin{bmatrix} I_m \\ 0 \end{bmatrix} h_2 + \begin{bmatrix} 0 \\ D_{s1} f_s \end{bmatrix} \\ w_3 &= [0 \quad I_{n-m}] q \end{aligned} \tag{2.21}$$

Consider that, the observability of (T_3, C_1) is implied given that C_1 is a full-rank matrix. Hence, the exitance of L_0 satisfying (2.19) is always guaranteed. To find a specific choice of L_0 the following Lemma is adopted from [54].

Lemma 2.1. *[54] The pair (A_z,C_z) is observable if the pair ($-T_3$,C_1) is detectable.*

Proof. For the proof please see [54]. □

Observability of (A_z,C_z) implies that there exists L_z such that $A_z - L_z C_z$ is Hurwitz. Therefore, the following Lyapunov equation can be stated

$$(A_z - L_z C_z)^T P_z + P_z(A_z - L_z C_z) = -Q_z \tag{2.22}$$

for positive definite matrices $Q_z \in \mathbb{R}^{2(n-m)\times 2(n-m)}$, and $P_z \in \mathbb{R}^{2(n-m)\times 2(n-m)}$. Now let

us, partition P_z and Q_z as in (2.23) and (2.24).

$$P_z = \begin{bmatrix} P_{z1} & P_{z2} \\ P_{z2}^T & P_{z3} \end{bmatrix} \tag{2.23}$$

$$Q_z = \begin{bmatrix} Q_{z1} & Q_{z2} \\ Q_{z2}^T & Q_{z3} \end{bmatrix} \tag{2.24}$$

Now, by substituting (2.23) and (2.24) into (2.22), it is easy to see that the following equation is hold:

$$(-T_3 + P_{z1}^{-1}P_{z2}C_1)^T P_{z1} + P_{z1}(-T_3 + P_{z1}^{-1}P_{z2}C_1) = -Q_{z1} \tag{2.25}$$

for details please refer to [54].

Now, the matrix gain L_0 can be obtained by comparing (2.25) and (2.19)as $L_0 = P_{z1}^{-1}P_{z2}$. By choosing such a L_0, (2.19) is readily satisfied, however to satisfy (2.20), we must have $L_0 D_{s1} = P_{z1}^{-1}P_{z2}D_{s1} = 0$, which is reduced to $P_{z2}D_{s1} = 0$. Therefore, P_{z2} can be obtained by parameterizing the null space of D_{s1} as:

$$P_{z2} = Z(I_{p-m} - D_{s1}(D_{s1}^T D_{s1})^{-1} D_{s1}^T) \tag{2.26}$$

where Z is a design parameter. Moreover, $(D_{s1}^T D_{s1})^{-1}$ always exists, since D_{s1} has full column rank.

The final form of transformed system is now given by: Subsystem 1:

$$\begin{cases} \dot{q}_1 = A_{q1}q_1 + A_{q2}q_2 + h_2 & \text{(2.27a)} \\ \dot{q}_2 = A_{q3}q_1 + A_{q4}q_2 + D_{s1}f_s & \text{(2.27b)} \\ w_3 = q_2 \end{cases}$$

Subsystem 2:

$$\begin{cases} \dot{h}_2 = \bar{f}(T^{-1}h) + \Delta f + g(T^{-1}h)(\tau + f_a) \\ \\ w_2 = C_4 h_2 \end{cases} \tag{2.28}$$

The following, now gives the summary of the design procedure:

1. First, solve the following LMI feasibility conditions satisfying (2.7) and (2.8) to get S_0 and D_{s1}.

$$C_s + C_s^T > \alpha I \tag{2.29}$$

$$C_4 + C_4^T > 0 \tag{2.30}$$

subject to

$$C_s C^{-1} D_s = [D_{s1}^T \quad 0]^T \tag{2.31}$$

where α is a positive scalar.

2. Get S_1 and T from (2.9) and (2.12).

3. Solve the following set of LMI feasibility conditions to find P_{z1} and P_{z2} such that (2.25) and (2.26) are satisfied.

$$(-T_3^T P_{z1} + C_1^T P_{z2}^T - P_{z1} T_3 + P_{z2} C_1) < 0 \tag{2.32}$$

subject to

$$P_{z2} = Z(I_{p-m} - D_{s1}(D_{s1}^T D_{s1})^{-1} D_{s1}^T) \tag{2.33}$$

Hence, the matrix L_0 satisfying (2.20) can be obtained as $L_0 = P_{z1}^{-1} P_{z2}$.

4. Find the design transformation matrix T_u from (2.17).

Note that in stage 1 of the above procedure, different selection of S_0 will affect the final form of matrices S and T given in (2.4). Therefore, the matrices C_1 and T_3 can be obtained by different selection of S_0. However, in selecting S_0, the result should yield in a Hurwitz A_{q1}, refer to the equation (2.21) which is important in designing a stable observer. Towards this end, we can obtain different solutions for S_0 by changing the constant α in (2.29) and therefore we can choose a stable solution for A_{q1}.

2.3 Conclusion

In this chapter, the required linear coordinate and output transformations to decompose the system into two subsystems have been presented. As a result, Subsystem 1 is affected by sensor faults only whereas Subsystem 2 is affected by actuator faults. Subsequently, an analytical approach has been presented to find coordinate transformation using LMI feasibility conditions. At last, in order to reconstruct the sensor fault associated with Subsystem 1, a new set of exo-states has been introduced such that the sensor faults enter the system equations as an unknown input.

Chapter 3

The Proposed Active Fault Accommodation Scheme Using Sliding Mode Observers

3.1 Introduction

Once the effects of sensor and actuator faults are separated, corresponding sensor and actuator fault estimation and reconstruction can be readily achieved using two sliding mode observers. The resulting fault estimations are then used to reconfigure the controller. Later in this chapter, the mathematical proof of stability for coupled controller, observers and nonlinear plant is demonstrated. Finally, simulation results performed on

a 3 DOF AUV are provided which reveals the effectiveness of our proposed FDIE and FTC schemes.

3.2 Sliding Mode Observer (SMO) Design

To summarize the results that we have obtained in the previous chapter, the original EL nonlinear system (1.25)-(1.26) can now be expressed as follows:

Subsystem 1:

$$\begin{cases} \dot{q}_1 = A_{q1}q_1 + A_{q2}q_2 + h_2 & \text{(3.1a)} \\ \dot{q}_2 = A_{q3}q_1 + A_{q4}q_2 + D_{s1}f_s & \text{(3.1b)} \\ w_3 = q_2 \end{cases}$$

Subsystem 2:

$$\begin{cases} \dot{h}_2 = \bar{f}(T^{-1}h) + \Delta f + g(T^{-1}h)(\tau + f_a) & \text{(3.2)} \\ w_2 = C_4 h_2 \end{cases}$$

where appropriate definitions for the matrices and the new states were given in Chapter 2. To estimate the sensor and actuator faults f_s and f_a, the following observers are now proposed.

Sensor fault observer:

$$\begin{cases} \dot{\hat{q}}_1 = A_{q1}\hat{q}_1 + A_{q2}w_3 + C_4^{-1}w_2 & \text{(3.3a)} \\ \dot{\hat{q}}_2 = A_{q3}\hat{q}_1 + A_{q4}\hat{q}_2 + L_1(w_3 - \hat{w}_3) + \nu_1 & \text{(3.3b)} \\ \hat{w}_3 = \hat{q}_2 \end{cases}$$

Actuator fault observer:

$$\begin{cases} \dot{\hat{h}}_2 = \bar{f}(T^{-1}\hat{h}) + g(T^{-1}\hat{h})\tau + \nu_2 \\ \hat{w}_2 = C_4\hat{h}_2 \end{cases} \tag{3.4}$$

where in (3.4), we have $\hat{h} = [\hat{h}_1^T \quad (C_4^{-1}w_2)^T]^T$, and $\hat{q} = [\hat{q}_1^T \quad \hat{q}_2^T]^T$. Therefore:

$$\hat{h}_1 \quad = \quad [I_{n-m} \quad 0]T_u^{-1}\hat{q} \tag{3.5}$$

Moreover, the matrix L_1 in (3.3b) denotes the observer gain designed to ensure the stability of the observer (specifically to guarantee that $A_{q4} - L_1$ is Hurwitz). Finally, we select the sliding terms ν_1 and ν_2 according to

$$\nu_1 \quad = \quad \begin{cases} \rho_1 \frac{P_{02}e_{q2}}{\|P_{02}e_{q2}\|}, & \text{if } e_{q2} \neq 0 \\ 0, & \text{otherwise} \end{cases} \tag{3.6}$$

$$\nu_2 \quad = \quad \begin{cases} \rho_2 \frac{e_{h2}}{\|e_{h2}\|}, & \text{if } e_{h2} \neq 0 \\ 0, & \text{otherwise.} \end{cases} \tag{3.7}$$

where $e_{q1} := q_1 - \hat{q}_1$, $e_{q2} := q_2 - \hat{q}_2$ and $e_{h2} := h_2 - \hat{h}_2$. The scalar functions ρ_1 and ρ_2 and the matrix P_{02} are to specified explicitly in the convergence proof of our main theorem stated next. The following theorem states the convergence of the above observers.

Theorem 3.1. *Given the dynamic model (3.1) and (3.2) subject to Assumptions 1 and 2, and the observer governed by (3.3) and (3.4); for any initial state $q(0)$, $h_2(0)$, $\hat{q}(0)$ and $\hat{h}_2(0)$ and any bounded input τ, there exist ν_1 and ν_2 expressed in (3.6) and (3.7), respectively, such that the observer states $\hat{q}$ and $\hat{h}_2$ converge in finite time to q and h_2 .*

Proof. The observation error dynamics can be obtained as:

$$\begin{cases} \dot{e}_{q1} = A_{q1} e_{q1} & \text{(3.8a)} \\ \dot{e}_{q2} = A_{q3} e_{q1} + (A_{q4} - L_1) e_{q2} + D_{s1} f_s - \nu_1 & \text{(3.8b)} \end{cases}$$

$$\begin{cases} \dot{e}_{h2} = (\bar{f}(T^{-1}h) - \bar{f}(T^{-1}\hat{h}) + (g(T^{-1}h) - g(T^{-1}\hat{h}))\tau \\ \qquad + g(T^{-1}h) f_a + \Delta f - \nu_2 \end{cases} \quad \text{(3.9)}$$

Let us now define a composite Lyapunov function candidate $V = V_1 + V_2$, where V_1 and V_2 correspond to Subsystems 1 and 2, respectively. The proof is now conducted in the following two steps:

1. Step 1: In (3.8), by using the selected transformation T_u, it is guaranteed that the matrix A_{q1} is Hurwitz. Hence, it is obvious that e_{q1} is an exponentially decaying signal. Next, according to [100], the decaying term e_{eq1} can be neglected for stability analysis of the error dynamics governing e_{eq2}. Moreover, let us define $A_{s2} = A_{q4} - L_1$. Therefore, by choosing a proper matrix L_1, then A_{s2} can also be guaranteed to be Hurwitz. Hence, the following Lyapunov equations can always be satisfied for any $Q_{02} > 0$ that is

$$A_{s2}^T P_{02} + P_{02} A_{s2} = -Q_{02} \quad \text{(3.10)}$$

Let us now consider a Lyapunov function candidate $V_1 = e_{q2}^T P_{02} e_{q2}$. Then, by taking the time derivative of V_1 along the trajectory of the error dynamics (3.8),

one may obtain:

$$\dot{V}_1 = -e_{q2}^T Q_{02} e_{q2} + 2e_{q2}^T P_{02}(D_{s1} f_s - \nu_1) \tag{3.11}$$

Now by defining ν_1 as in (3.6) we get

$$\dot{V}_1 \leq -\lambda_{minQ02}\|e_{q2}\|^2 + 2\|e_{q2}\|\|P_{02}\|(\|D_{s1}\|\bar{f}_s) - \rho_1) \tag{3.12}$$

Now, by choosing $\rho_1 > \|D_{s1}\|\bar{f}_s$, it is straightforward to guarantee that ideal sliding motion takes place in finite time and therefore, the observation error (3.8) converges to zero in finite time. The finite time convergence property of the SMO will also be used in Step 2 of the proof [49].

2. Step 2: The dynamics (3.9) which describes the observation error h_2 is first re-written as follows:

$$\dot{e}_{h2} = F(h, \hat{h}, t) + g(T^{-1}h) f_a + \Delta f - \nu_2 \tag{3.13}$$

where $F(h, \hat{h}, t) = \bar{f}(T^{-1}h) - \bar{f}(T^{-1}\hat{h}) + (g(T^{-1}h) - g(T^{-1}\hat{h}))\tau$. Note that, the nominal system is stable and the faults do not destabilize the system or a singularity avoidance algorithm is applied. Hence, we can conclude that the states are bounded and therefore accelerations in the mechanical system remain bounded (This will be shown later in the proof of Theorem 3.2 in this chapter). Further, considering the result of Step 1 which shows the boundedness of $\hat{h}_1$ and given that the

actual measured state h_2 is also bounded, we can infer both h and $\hat{h}$ are bounded. Consequently by considering the properties of EL system, we can conclude that $\bar{f}(T^{-1}h)$, $\bar{f}(T^{-1}\hat{h})$, ($g(T^{-1}h)$ and $g(T^{-1}\hat{h})$ are bounded. Therefore, in overall we guaranteed that, the constant f^+ can be found, such that $\|F(h,\hat{h},t)\|< f^+$. Moreover, $F(h,\hat{h},t)$ converges to zero in finite time, due to convergence of $\hat{h}$ to h in finite time.

Let us now consider $V_2 = e_{h2}^T e_{h2}$, where the time derivative of V_2 along the trajectory of the error dynamics (3.9) yields:

$$\dot{V}_2 = e_{h2}^T(F(h,\hat{h},t) + g(T^{-1}h)f_a + \Delta f - \nu_2) \tag{3.14}$$

Now, substitute for ν_2 from (3.7) into (3.14):

$$\dot{V}_2 = e_{h2}^T(F(h,\hat{h},t) + g(T^{-1}h)f_a + \Delta f - \rho_2\frac{e_{h2}}{\|e_{h2}\|}) \tag{3.15}$$

$$\leq \|e_{h2}\|(\|F(h,\hat{h},t)\|+\|g(T^{-1}h)\|\|f_a\|+\|\Delta f\|-\rho_2) \tag{3.16}$$

Considering the upper bound of actuator fault, disturbances, uncertainties, and also having $\|F(h,\hat{h},t)\|< f^+$, one can conclude that:

$$\dot{V}_2 \leq \|e_{h2}\|(f^+ + \|g(T^{-1}h)\|_{max}\bar{f}_a + \Delta\bar{f} - \rho_2) \tag{3.17}$$

Thus, by choosing $\rho_2 > f^+ + \|g(T^{-1}h)\|_{max}\bar{f}_a + \Delta\bar{f}$, it now follows that $\dot{V}_2 < 0$, therefore, in this case finite time convergence can take place for Step 2 as well.

Note that, in this case $\|g(T^{-1}h)\|_{max}$ is the maximum norm of $g(T^{-1}h)$ which amounts to the inverse of the inertia matrix, which is known to be bounded based on the Property 2.

By considering the above two steps, the time derivative of V along the trajectories of the error dynamics (3.8) and (3.9) can be ensured to be negative definite as well and the observation errors e_{q1}, e_{q2} and e_{h2} all converge to zero in finite time. This complete the proof of the theorem. □

Based on the above convergence analysis, one can now conclude that the observation errors slide along the manifold $e = 0$, and hence the states of EL system as well as the fault signal can be accurately estimated.

3.3 Online Robust Fault Reconstruction

In this section, the finite time convergence of the observers will be used to estimate the severity of the faults. As will be shown subsequently, the faults f_s and f_a can also be estimated in finite time. Hence, these estimates will be served as the residual signals for fault detection and isolation purposes. In fact, the value of each elements of the fault vectors estimates can determine if and where the fault has occurred in the system. Hence, we can perform and accomplish fault detection, isolation, and estimation all in one stage based on the estimated values of f_s and f_a, respectively.

Therefore, once the observer states have reached their sliding surfaces and converged to the actual values of EL system states, in finite time we have $e_{q1} = 0$, $e_{q2} = 0$, $e_{h2} = 0$ and $\dot{e}_{q1} = 0$, $\dot{e}_{q2} = 0$, $\dot{e}_{h2} = 0$. Therefore, by considering (3.8b), the following condition can be ensured,

$$0 = D_{s1} f_s - \nu_1$$

Hence, it can be concluded that the estimation of sensor fault can be obtained from

$$\begin{aligned} \hat{f}_s &= ((D_{s1})^T D_{s1})^{-1} D_{s1}^T \nu_{eq1} \\ \nu_{eq1} &= \rho_1 \frac{P_{02} e_{q2}}{\|P_{02} e_{q2}\| + \delta} \end{aligned} \tag{3.18}$$

where $((D_{s1})^T D_{s1})^{-1} D_{s1}^T$ is the pseudo inverse of D_{s1} and its existence is guaranteed since D_{s1} has a full column rank. Moreover, to prevent division by zero in implementing (3.6), we have used a continuous approximation for the discontinuity of ν_1, denoted by ν_{eq1} by adding a small positive number δ to the denominator of ν_1 as given above.

Furthermore, considering equation (3.13), we also obtain:

$$0 = g(T^{-1}h) f_a + \Delta f - \nu_2$$

Hence, the estimate of the actuator fault can be obtained from

$$\begin{aligned} \hat{f}_a &= g(T^{-1}h)^{-1} (\nu_{eq2} - \Delta \bar{f}) \\ \nu_{eq2} &= \rho_2 \frac{e_{h2}}{\|e_{h2}\| + \delta} \end{aligned} \tag{3.19}$$

where we have used the sigmoid function as an approximation of ν_2.

Note that in (3.19), the term $\Delta\bar{f}$ represents the upper bound of the uncertainties, unmodeled dynamics and disturbances in the system. We should emphasize that in the presence of large uncertainties and disturbances, even though the estimation accuracy is degraded, the observers would still maintain their overall stability property.

However, measurement noise,uncertainties and disturbances can influence and affect the estimated fault severity. Therefore, a thresholding mechanism is required to robustly declare a fault. One can use the Monte Carlo simulation in selecting the proper choice of the thresholds.

3.4 The Active Fault Accommodation Methodology

The idea of fault recovery in this work, is to use the result of fault estimation obtained from the observer blocks. The controller reconfiguration scheme is presented in Figure 3.1.

Firstly, we investigate the stability of the closed-loop system, in the faultless scenario and review the stability proof from [97]. Next, the proposed fault accommodation strategy is stated. Thereupon, we will investigate the stability of the closed-loop system with the proposed fault accommodation scheme in the presence of simultaneous sensor and actuator faults. Finally, a comparative study is provided to evaluate tracking performance with and without the proposed fault accommodation methodology as compared to the FDIE strategy proposed in [60].

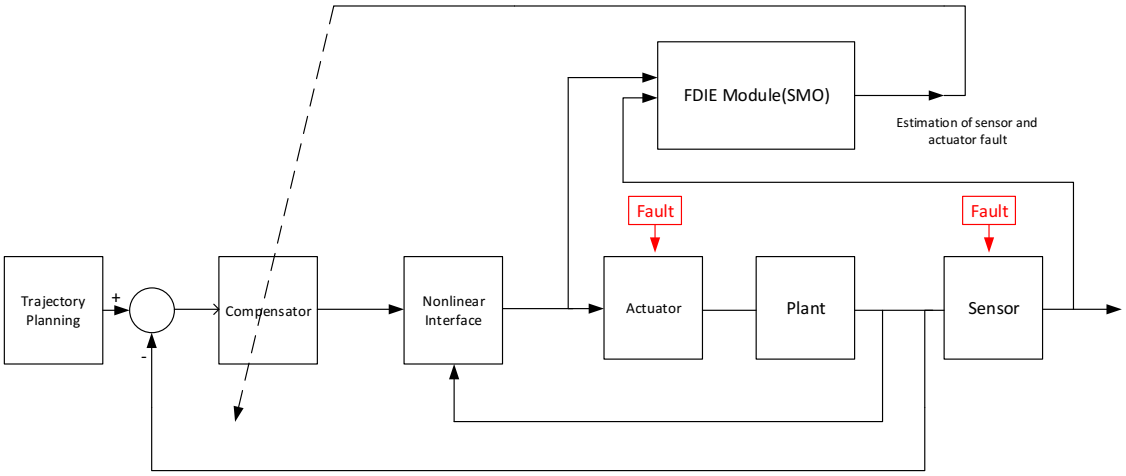

Figure 3.1: The schematic of the proposed active fault reconfiguration scheme

Inverse dynamics is a popular method for trajectory tracking in systems governed by EL equations. In this method, two loops should be designed. In the inner loop, the nonlinearity of the system is canceled using inverse dynamics and in the outer loop the tracking controller is designed for the resulting linear system [97]. Figure 3.2 illustrates the inverse dynamics control structure.

For a rigid body, governed by (1.23), the inner loop controller is in the form of:

$$\tau = M(x_1)aq + C_{co}(x_1, x_2)x_2 + G(x_1) \tag{3.20}$$

Since the inertia matrix is invertible, this control input results in the following closed-loop dynamic equation:

$$\dot{x}_2 = aq + \Delta f \tag{3.21}$$

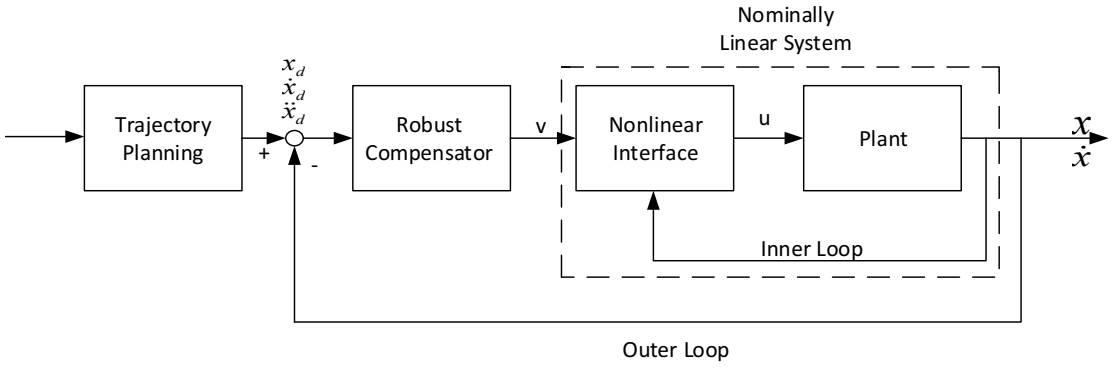

Figure 3.2: The schematic of inverse dynamics control scheme [97]

The closed-loop system dynamics (3.21) is linear, therefore many well defined control techniques exist to stabilize the system. Let us define $x_d(t)$, $\dot{x}_d(t)$, and $\ddot{x}_d(t)$ as desired position, velocity and acceleration of the system, respectively. Hence, aq can be defined follows:

$$aq \quad = \quad \ddot{x}_d(t) - K_0\tilde{x} - K_1\dot{\tilde{x}} \tag{3.22}$$

where $\tilde{x} = x_1 - x_d$, $\dot{\tilde{x}} = x_2 - \dot{x}_d(t)$, K_0 and K_1 are diagonal matrices corresponding to position and velocity gains, respectively. This controller is basically a PD control with feedforward acceleration. Substituting (3.22) into (3.21), the closed-loop error dynamics can be obtained as follows:

$$\ddot{\tilde{x}}(t) + K_1\dot{\tilde{x}} + K_0\tilde{x} \quad = \quad \Delta f$$

This error equation is clearly a stable system for all positive K_0 and K_1 in the presence of smooth, bounded and relatively small uncertainties.

Now, consider the rigid body dynamics given in (1.23) with added sensor and actuator faults:

$$\begin{cases} \dot{x}_1 = x_2 \\ \dot{x}_2 = M^{-1}(x_1)((\tau + f_a) - C_{co}(x_1, x_2)x_2 - G(x_1)) + \Delta f \end{cases} \tag{3.23}$$

$$y = Cx + D_s f_s \tag{3.24}$$

In the presence of sensor and actuator faults, we can use the results of the proposed observers and accommodate the controller such that the effects of faults is reduced. To compensate the effect of the faults in the system, the scheme illustrated in Figure 3.1 is proposed. In this methodology, estimated values of the sensor and actuator faults obtained from SMOs are used.

Basically, in order to realize the control signal, we need to find the correct state values from the faulty measured output. From (1.26), which describes the output equation of our system, we can obtain:

$$x = C^{-1}(y - D_s f_s) \tag{3.25}$$

In (3.25), f_s is unknown. Therefore, the estimation of the sensor fault found in (3.18), can be used to estimate the correct values of the states. Hence, the estimated state can be given by:

$$\hat{x} = [\hat{x}_1^T \quad \hat{x}_2^T]^T = C^{-1}(y - D_s \hat{f}_s) \tag{3.26}$$

In this work, we propose the following control input:

$$\tau = M(\hat{x}_1)aq + C_{co}(\hat{x}_1, \hat{x}_2)\hat{x}_2 + G(\hat{x}_1) - \hat{f}_a \tag{3.27a}$$

$$aq = \ddot{x}_d(t) - K_0(\hat{x}_1 - x_d(t)) - K_1(\hat{x}_2 - \dot{x}_d(t)) \tag{3.27b}$$

The following theorem concerns the stability of the closed-loop system using the above control input.

Theorem 3.2. *Consider the closed-loop system illustrated in Figure 3.1, where the plant is an EL system modeled by (3.23)-(3.24) affected by simultaneous sensor and actuator faults, the observers are given in (3.3) and (3.4), and the control input is given by (3.27). Then, Under Assumptions 1 and 2, the control reconfiguration scheme can maintain the closed-loop system stability in the presence of simultaneous sensor and actuator faults.*

Proof. Before getting into the details of the proof, we present an outline:

- Step 1: Given (3.18) and (3.19), first we can easily show that the estimates of actuator and sensor faults are bounded.

- Step 2: We show that the closed-loop error dynamics can be expressed as linear dynamics subject to a nonlinear term consisting uncertainties and faults.

- Step 3: Considering the properties of EL systems, We show that the nonlinear term mentioned above is bounded by position and velocity tracking errors. Then we conclude that the tracking error is bounded in presence of bounded actuator and sensor fault estimation errors.

- Step 4: Having shown the boundedness of tracking error, we can infer that the estimated actuator and sensor faults converge to their respective true values in **finite time**.

Based on the outline above, we have the following steps in our proof:

- Step 1: First, considering (3.18) and (3.19), we can see that the estimation of sensor and actuator faults obtained from the observers are always bounded with the upper bounds ρ_1 and ρ_2 for sensor and actuator faults, respectively. In other words, since in the estimation of the sensor and actuator faults we have the observation error over is magnitude, even if the stability of the observers is compromised, the fault estimation signals sent to the controller and therefore affect the closed-loop stability, is bounded. Moreover, based on Assumption 2, the actual sensor and actuator faults are also bounded. Hence, we can conclude that $f_a - \hat{f}_a$ and $f_s - \hat{f}_s$ are bounded.

Hence, in the first place, if we use $\hat{x} = C^{-1}(y - D_s\hat{f}_s)$ as the estimation of states of the system, we have:

$$\Delta x \quad = \quad x - \hat{x} = C^{-1}D_s(f_s - \hat{f}_s) \tag{3.28}$$

Therefore, it can be easily seen, that Δx, which represents state estimation error, is bounded.

• Step 2: Based on [101], we define $H(x_1, x_2) = C_{co}(x_1, x_2)x_2$. Moreover, substituting the control input (3.27a) into (3.23) results in:

$$\begin{aligned} M(x_1)\dot{x}_2 &= M(\hat{x}_1)aq + (H(\hat{x}_1, \hat{x}_2) - H(x_1, x_2)) \\ &+ (G(\hat{x}_1) - G(x_1)) + (f_a - \hat{f}_a) + \Delta f \end{aligned} \tag{3.29}$$

Now by adding and subtracting the term $M(x_1)aq$ to the right hand side of (3.29), we obtain:

$$M(x_1)(\dot{x}_2 - aq) = \eta \tag{3.30}$$

where

$$\begin{aligned} \eta &= (M(\hat{x}_1) - M(x_1))aq + (H(\hat{x}_1, \hat{x}_2) - H(x_1, x_2)) \\ &+ (G(\hat{x}_1) - G(x_1)) + (f_a - \hat{f}_a) + \Delta f \end{aligned} \tag{3.31}$$

Then, by substituting aq from (3.27b) into(3.30) and considering (3.28), the tracking error dynamics of the closed-loop system in the presence of simultaneous sensor and actuator faults can be expressed as follows:

$$\ddot{\tilde{x}}(t) + K_1\dot{\tilde{x}} + K_0\tilde{x} = M(x_1)^{-1}\eta + \epsilon = \zeta \tag{3.32}$$

where

$$\epsilon = K_1\Delta x_2 + K_0\Delta x_1 \tag{3.33}$$

Now, similar to the analysis given in [102], we define the following transfer functions

M_i from each position error and N_i from each velocity errors. Then, we have:

$$\frac{\tilde{x}_i(s)}{\zeta_i(s)} = M_i(s) = \frac{1}{s^2 + K_{1i}s + K_{0i}} \tag{3.34}$$

$$\frac{\dot{\tilde{x}}_i(s)}{\zeta_i(s)} = N_i(s) = \frac{s}{s^2 + K_{1i}s + K_{0i}} \tag{3.35}$$

It can be easily seen that both transfer functions are stable and their corresponding L_∞ gains are bounded. Therefore, we can write

$$\|\tilde{x}\|_{T\infty} = a_1\|\zeta\|_{T\infty} \tag{3.36}$$

$$\|\dot{\tilde{x}}\|_{T\infty} = a_2\|\zeta\|_{T\infty} \tag{3.37}$$

where a_1 and a_2 are bounds on operators M and N respectively, and $\|.\|_{T\infty}$ denotes the L_∞ norm at **truncated time** T. From (3.36) and (3.37), we can conclude that $\zeta \in L_\infty$ results in $\tilde{x}, \dot{\tilde{x}} \in L_\infty$.

• Step 3: Using a similar approach to that given in [102], we can show that ζ is bounded by the position and velocity tracking errors and under some reasonable conditions on system parameters, both position and velocity tracking errors are bounded. Towards this end, let us consider each term of η and ϵ.

First, considering Property 2, we can conclude that the inertia matrix is bounded and therefore the matrix $M(x_1)^{-1}$ is bounded as well.

Then, let us consider the first term in η which is $(M(\hat{x}_1) - M(x_1))aq$. This term also contains inertia matrix. Since inertia matrix is containing trigonometric functions

such as sine and cosine function, both $M(\hat{x}_1)$ and $M(x_1)$ and therefore their difference are bounded.

Moreover, aq, which is defined in (3.27b) consists of three terms itself. The first term $\ddot{x}_d(t)$ is a bounded term, since this term represents the desired bounded acceleration. The other two terms are clearly bounded by position and velocity errors. Hence, in overall, for the first term of η, we have:

$$\|(M(\hat{x}_1) - M(x_1))aq\| \quad \leq \quad \gamma_{11} + \gamma_{21}\|\tilde{x}\| + \gamma_{31}\|\dot{\tilde{x}}\| \tag{3.38}$$

where γ_is are scalars constant.

Moreover, the third term of η, which is $(G(\hat{x}_1) - G(x_1))$, is also bounded based on Property 3 and can be expressed as:

$$\|(G(\hat{x}_1) - G(x_1))\| \quad \leq \quad \gamma_{12} \tag{3.39}$$

The forth and fifth terms of η which are $(f_a - \hat{f}_a) + \Delta f$, are also bounded based on the reasoning given in Step 1 and can be expressed as:

$$\|(f_a - \hat{f}_a) + \Delta f\| \quad \leq \quad \gamma_{13} \tag{3.40}$$

However, in order to analyze the second term, we need to consider (3.28) in order to express $\hat{x} = x + \Delta x$. Therefore, we can rewrite $(H(\hat{x}_1, \hat{x}_2) - H(x_1, x_2))$, as $(H(x_1 + \Delta x_1, x_2 + \Delta x_2) - H(x_1, x_2))$. Thereupon, using Taylor series expansion for the term

$H(x_1 + \Delta x_1, x_2 + \Delta x_2)$ at (x_1, x_2), we have:

$$\begin{aligned} H \quad & (x_1 + \Delta x_1, x_2 + \Delta x_2) - H(x_1, x_2) = H(x_1, x_2) + \frac{\partial H}{\partial x_1}(x_1, x_2)\Delta x_1 \\ + \quad & \frac{\partial H}{\partial x_2}(x_1, x_2)\Delta x_2 + \frac{\partial^2 H}{\partial x_1^2}(x_1, x_2)\Delta x_1^2 + \frac{\partial^2 H}{\partial x_2^2}(x_1, x_2)\Delta x_2^2 \\ + \quad & \frac{\partial^2 H}{\partial x_1 \partial x_2}(x_1, x_2)\Delta x_1 \Delta x_2 + H.O.T - H(x_1, x_2) \end{aligned} \tag{3.41}$$

Since the Coriolis matrix consists of quadratic terms of the velocities, we can conclude that in $H.O.T$, the higher order derivatives with respect to velocities are equal to zero and the higher order derivatives with respect to positions are sine and cosine functions. Since, Δx_1 and Δx_2 which are state estimation errors defined in (3.28) are bounded, the upper bound of $H(\hat{x}_1, \hat{x}_2) - H(x_1, x_2)$ can be expressed as follows:

$$\|H(\hat{x}_1, \hat{x}_2) - H(x_1, x_2)\| \quad \leq \quad \gamma_{14} + \gamma_{22}\|\tilde{x}\| + \gamma_{32}\|\dot{\tilde{x}}\| + \gamma_4\|\dot{\tilde{x}}\|^2 \tag{3.42}$$

Furthermore, the term ϵ in (3.32) which is defined in (3.33) is bounded, since Δx_1 and Δx_2 are bounded and K_1 and K_2 are constant matrices. Therefore, we have:

$$\|\epsilon\| \quad \leq \quad \gamma_{15} \tag{3.43}$$

Now, by substituting (3.38), (3.39), (3.40), (3.42), and (3.43) in (3.32), we can write:

$$\|\zeta\| \quad \leq \quad \gamma_1 + \gamma_2\|\tilde{x}\| + \gamma_3\|\dot{\tilde{x}}\| + \gamma_4\|\dot{\tilde{x}}\|^2 \tag{3.44}$$

where, $\gamma_1 = \gamma_{11} + \gamma_{12} + \gamma_{13} + \gamma_{14} + \gamma_{15}$, $\gamma_2 = \gamma_{21} + \gamma_{22}$, and $\gamma_3 = \gamma_{31} + \gamma_{32}$. Next, combining

(3.36), (3.37), and (3.44) leads to the following inequalities:

$$\|\tilde{x}\| \leq \frac{a_1\gamma_1}{1-a_1\gamma_2} + \frac{a_1\gamma_3}{1-a_1\gamma_2}\|\dot{\tilde{x}}\| + \frac{a_1\gamma_4}{1-a_1\gamma_2}\|\dot{\tilde{x}}\|^2 \tag{3.45}$$

$$\|\tilde{x}\| \geq \frac{-\gamma_1}{\gamma_2} + \frac{1-a_2\gamma_3}{a_2\gamma_2}\|\dot{\tilde{x}}\| + \frac{-\gamma_4}{\gamma_2}\|\dot{\tilde{x}}\|^2 \tag{3.46}$$

To determine a closed region on magnitude plane where bounds the position and velocity errors, the two quadratic expressions in (3.45) and (3.46) should intersect. Therefore, if we equate (3.45) and (3.46), another quadratic expression is found which should have two real roots.This condition is equivalent to have positive discriminant which leads to the following inequality:

$$a_1\gamma_2 + a_2\gamma_3 + 2a_2\sqrt{\gamma_1\gamma_4} \leq 1 \tag{3.47}$$

Note that, in (3.47), a_1 and a_2 are the design parameters. Hence, by proper selection of K_0 and K_1, this inequality can be satisfied.

Therefore, if (3.47) is satisfied, position and velocity tracking errors are bounded and we have $\tilde{x} \in L_\infty$ and $\dot{\tilde{x}} \in L_\infty$

• Step 4: Once the boundedness of the states is guaranteed, we can conclude that the observers introduced in (3.3) and (3.4) have bounded inputs w_2, w_3, and τ. Based on the analysis given in Section 3.2, the states of the SMO given in (3.3) and (3.4) converges to the true values of system states in finite time.

Therefore, the estimated values of sensor and actuator faults converge to their corresponding actual values in **finite time**. once the true values of the faults have been

obtained and fed back to the inverse dynamics controller (3.27), the following tracking error dynamics is obtained which clearly represents a stable linear dynamics subject to bounded input.

$$\ddot{\tilde{x}}(t) + K_1\dot{\tilde{x}} + K_0\tilde{x} \quad = \quad M(x_1)^{-1}\Delta f \tag{3.48}$$

□

3.5 Simulation Results

To evaluate the performance of our proposed fault detection, isolation and estimation strategy, a set of simulations are performed below on an Autonomous Underwater Vehicle (AUV) modeled by EL equations as in (1.23). In this simulation, the dynamic equations represent the lateral motions of an AUV with three actuators, the numerical parameters of which are adopted from [103]. The state variables for lateral motions are considered as $X = [x \quad y \quad \psi \quad \dot{x} \quad \dot{y} \quad \dot{\psi}]^T$, where x and y denote body position coordinates in an Earth-fixed reference frame and ψ denotes the Euler angle coordinates, corresponding to the rotation about the z axis in the same reference frame. The input vector τ is also defined as the torque applied to the AUV. The corresponding numerical value of the

AUV model are given below:

$$M_V = \begin{bmatrix} 80.026 & 0 & 0 \\ 0 & 50.041 & 0.0139 \\ 0 & 0.0139 & 10.011 \end{bmatrix}, \tag{3.49}$$

$$N_V = \begin{bmatrix} 0.72 & 0 & 0 \\ 0 & 0.8896 & 7.25 \\ 0 & 0.0313 & 1.9 \end{bmatrix}, \tag{3.50}$$

$$C_{coV} = \begin{bmatrix} 0 & 0 & -(80.041v + 0.0139r) \\ 0 & 0 & 80.026u \\ 80.041v + 0.0139r & -80.026u & 0 \end{bmatrix} \tag{3.51}$$

where u and v denote the linear velocity expressed in the Earth-fixed frame in the x and y directions, respectively. Moreover, r denotes the angular velocity expressed in the body-fixed frame.

Furthermore, the output matrix given by $C = I_6$, and the sensor fault distribution matrix is given by $D_s = [0 \quad -1 \quad 0 \quad 0 \quad 1 \quad 0]^T$.

Corresponding to the above AUV model, the matrix S_0 associated with the output

redefinition matrix is obtained as follows:

$$S_0 = \left[\begin{array}{cccccc} 1.43 & 0 & 0 & 0 & 0 & 0 \\ 0 & 1.07 & -0.26 & 0 & 0.07 & 0.74 \\ 0 & -0.26 & 1.74 & 0 & 0.74 & -0.25 \\ 0 & 0 & 0 & 1.43 & 0 & 0 \\ 0 & 1.15 & -0.15 & 0 & 1.15 & -0.15 \\ 0 & -0.15 & -0.25 & 0 & -0.15 & 1.56 \end{array}\right] \tag{3.52}$$

Using this matrix, we have:

$$S_0 C = S_0 \tag{3.53}$$

$$S_0 D_s = [0 \quad -1 \quad 1 \quad 0 \quad 0 \quad 0]^T \tag{3.54}$$

Therefore, the matrix S_1 and T are obtained according to:

$$S_1 = \begin{bmatrix} 1 & 0 & 0 & 0 & 0 & 0 \\ 0 & 1 & 0 & 0 & -0.1243 & -0.4863 \\ 0 & 0 & 1 & 0 & -0.6305 & 0.0996 \\ 0 & 0 & 0 & 1 & 0 & 0 \\ 0 & 0 & 0 & 0 & 1 & 0 \\ 0 & 0 & 0 & 0 & 0 & 1 \end{bmatrix}, \tag{3.55}$$

$$T = \begin{bmatrix} 1 & 0 & 0 & 0 & 0 & 0 \\ 0 & 1 & 0 & 0 & 0 & 0 \\ 0 & 0 & 1 & 0 & 0 & 0 \\ 0 & 0 & 0 & 1 & 0 & 0 \\ 0 & 1 & -0.1533 & 0 & 1 & 0 \\ 0 & 0 & -0.1750 & 0 & 0 & 1 \end{bmatrix} \tag{3.56}$$

Moreover, the following matrix for T_u is selected according to (2.17), (2.32) and (2.33):

$$T_u = \begin{bmatrix} 1 & 0 & 0 & -5.0791 & -0.0003 & -0.0003 \\ 0 & 1 & 0 & -0.0004 & -6.9364 & -6.9364 \\ 0 & 0 & 1 & -0.0003 & -8.7428 & -8.7428 \\ 0 & 0 & 0 & 1 & 0 & 0 \\ 0 & 0 & 0 & 0 & 1 & 0 \\ 0 & 0 & 0 & 0 & 0 & 1 \end{bmatrix} \tag{3.57}$$

In simulations conducted below, the zig-zag maneuver is considered which is a standard trajectory used to compare the maneuvering properties and control characteristic of an AUV [99]:

$$X_d = \begin{bmatrix} 9\cos(t/9) \\ t/3 \\ \pi/6 \end{bmatrix} \tag{3.58}$$

Moreover, the sensor faults are modeled according to:

$$f_s = \begin{cases} 0, & t < 40; \\ (0.3t) - 12, & 40 \leq t < 50; \\ 3, & t \geq 50. \end{cases} \tag{3.59}$$

Considering the sensor fault distribution matrix D_s, the measurement of x_2 and x_5 are subjected to faults occurring at $t = 40second$. Thereafter, the sensor faults are followed by the actuator faults modeled as additive bias where $f_a = [f_{a1} \quad f_{a2} \quad f_{a3}]^T$ described in (3.60) to (3.62). In this scenario, the first, second and third actuators become faulty at $t = 45second$, $t = 55second$, and $t = 65second$, respectively .

$$f_{a1} = \begin{cases} 0, & t < 45; \\ 1, & t \geq 45. \end{cases} \tag{3.60}$$

$$f_{a2} = \begin{cases} 0, & t < 55; \\ 2, & t \geq 55. \end{cases} \tag{3.61}$$

$$f_{a3} = \begin{cases} 0, & t < 65; \\ 0.01, & t \geq 65. \end{cases} \tag{3.62}$$

Using the proposed methodology, the fault estimation results are illustrated in Figures 3.3 and 3.4. The results given in these figures illustrate that the sensor and actuator faults are successfully estimated utilizing our proposed method. As can be seen, the estimated faults show the zero error during the fault free interval (i.e., $t \leq 40 second$ in Fig. 3.3 and $t \leq 45 second$ in Fig. 3.4). At the instant that the fault is injected and starts to build up, the estimators promptly react and estimate the true value of the fault in negligible transient time.

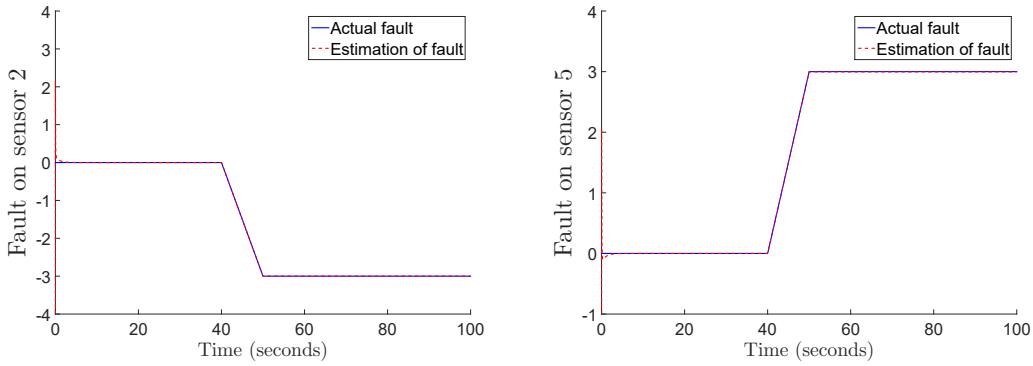

(a) The result for position sensor 2.

(b) The result for velocity sensor 2.

Figure 3.3: Simulation results for sensor fault estimation: the actual and estimated values of f_s.

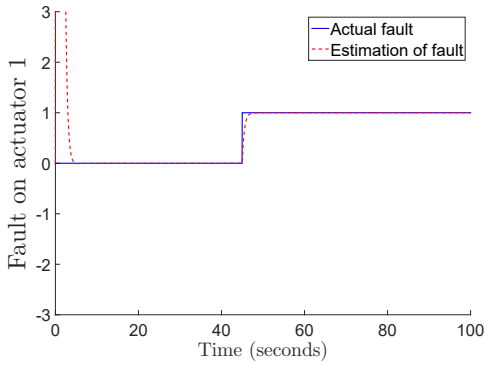

(a) The result for actuator 1.

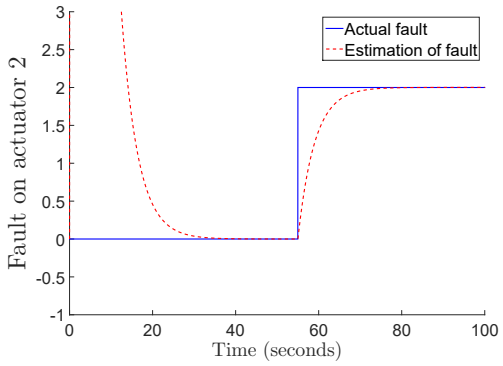

(b) The result for actuator 2.

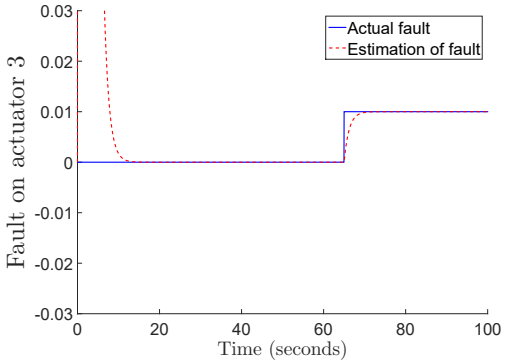

(c) The result for actuator 3.

Figure 3.4: Simulation results for actuator fault estimation: the actual and estimated values of f_a.

However, it should be noted that, the fault estimation results will be affected by the measurement noise, modeling uncertainties and disturbances. Therefore, to evaluate the performance of the proposed fault detection and isolation strategy, a Monte Carlo simulation was performed. We have run the simulation for 40 times. The uncertainty and disturbances used in the simulation is modeled by Δf in dynamic model (1.24). In this simulation, since the plant is an AUV, the disturbance is considered as the ocean current, the details of which is presented in Section 1.4.1. The initial condition for the dynamics of the disturbance (1.20) is set to $[1 \quad 1 \quad 0]^T$.

Moreover, the measurement noise is considered as a band-limited white noise with normal distribution and power (height of power spectral density) of 0.01. The results are represented graphically as shown in Figures 3.5 and 3.6.

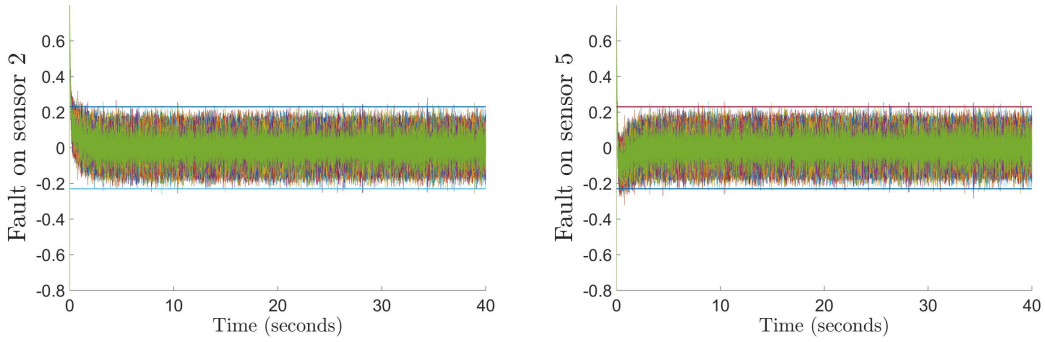

(a) The result for position sensor 2.

(b) The result for velocity sensor 2.

Figure 3.5: The result of Monte Carlo simulations performed for proper threshold setting for sensor fault estimation.

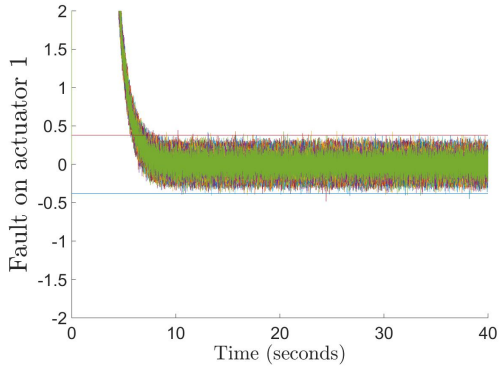

(a) The result for actuator 1.

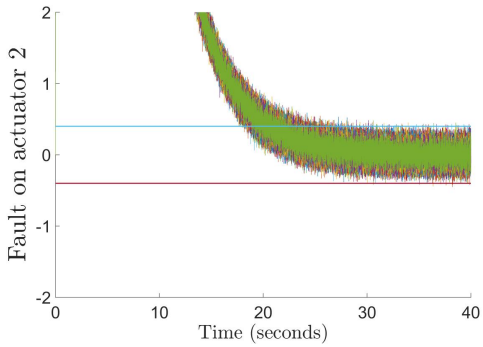

(b) The result for actuator 2.

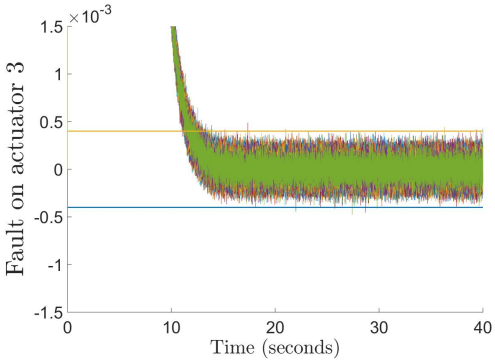

(c) The result for actuator 3.

Figure 3.6: The result of Monte Carlo simulations performed for proper threshold setting for actuator fault estimation.

f_{a1}	f_{a2}	f_{a3}	f_{s1}	f_{s2}
0.4	0.45	0.0004	0.25	0.26

Table 3.1: Fault detection thresholds found using Monte Carlo simulations

Monte Carlo simulation can be used to obtain a proper threshold level based on the property of the noise and uncertainty in the system. The suggested threshold level for each channel is given in Table 3.1. Hence, any faults with severity greater than the threshold level is detectable. We can see that the threshold for each fault in each channel is different. Monte Carlo simulation results confirm this fact.

However, if the amplitude of the noise and the disturbance are increased by 10%, then the accuracy of the proposed methodology can be evaluated by another Monte Carlo simulation, the result of which is presented in the Confusion matrix given in Table 3.2. The rows of this array show the location of the injected fault, whereas the columns indicate the location of the estimated faults. For instance, the first row shows that out of 40 times that the first actuator was faulty, 34 times the fault was properly isolated while in 6 other simulations the location of the fault was mistakenly determined.

Moreover, in Figure 3.7 and 3.8 sensor and actuator fault estimation results are given in the presence of measurement noises, respectively. It can be seen that both faults are also estimated correctly.

In the next simulation, a comparative study has been performed to evaluate the

	$\hat{f}_{a1}$	$\hat{f}_{a2}$	$\hat{f}_{a3}$	$\hat{f}_{s1}$	$\hat{f}_{s2}$
f_{a1}	34	1	3	0	2
f_{a2}	1	32	1	3	3
f_{a3}	0	0	38	1	1
f_{s1}	0	1	1	34	4
f_{s2}	0	0	1	2	37

Table 3.2: The confusion matrix resulting from Monte Carlo simulations

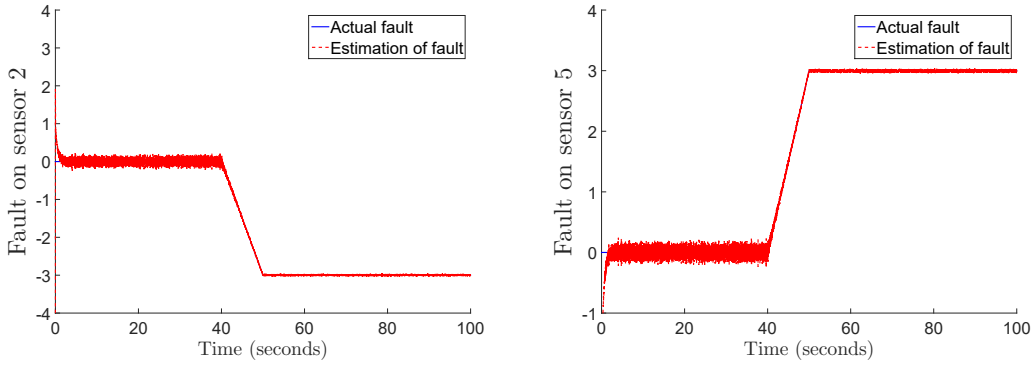

(a) The result for position sensor 2.

(b) The result for velocity sensor 2.

Figure 3.7: Simulation results for sensor fault estimation in the presence of measurement noises: the actual and estimated values of f_s.

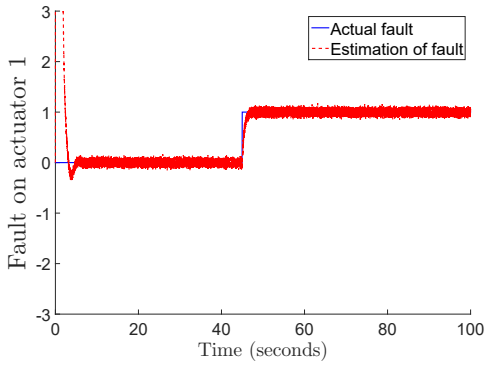

(a) The result for actuator 1.

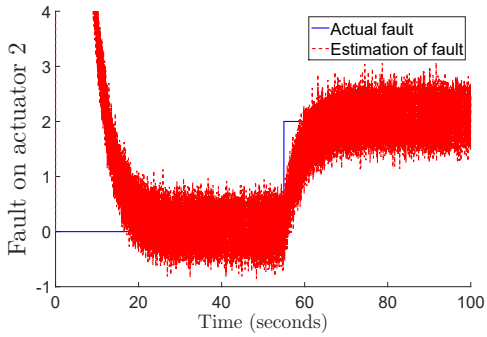

(b) The result for actuator 2.

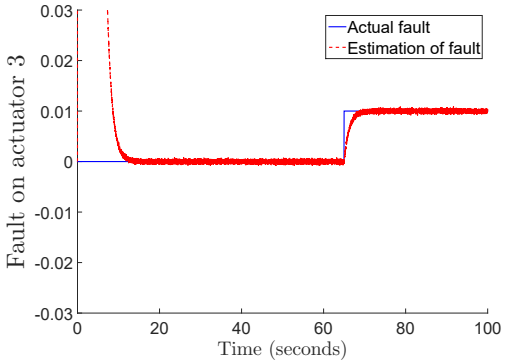

(c) The result for actuator 3.

Figure 3.8: Simulation results for actuator fault estimation in the presence of measurement noises: the actual and estimated values of f_a.

performance of the FDIE methodology proposed in this work and that of [60]. It is worth mentioning that in the previous work on estimation of simultaneous sensor and actuator faults for nonlinear system [60], the nonlinearity is just considered as a Lipschitz additive term. Moreover, the input matrix was slao assumed to be linear. However, for Euler-Lagrange system the input matrix is also nonlinear. Therefore, to apply this methodologies for EL systems, the input matrix needs to be linearized. Figure 3.9-Figure 3.12 compares the performances of the two FDIE schemes, in the presence of faults with different severities. It can be seen that linearization significantly degrades estimation accuracy and detection sensitivity. In other words, if the fault amplitude decreases, the accuracy and sensitivity of our nonlinear approach vs the methodology proposed in [60] become more clear. One the other hand, our proposed methodology uses the nonlinear input matrix which is natural to be computationally expensive. However, the complexity is due to the nonlinear nature of the approach and there is no added complexity.

Furthermore, the results of fault recovery scheme are illustrated in Figure 3.13-3.14.

From these figures, we can see that in the presence of faults, zero steady state error is not obtainable if the controller is not reconfigured. However, using the online recovery methodology proposed in this work, the results are significantly improved and smaller tracking error is obtained. As demonstrated in the figures, the convergence is smooth i.e. with reasonable settling time and small overshoot.

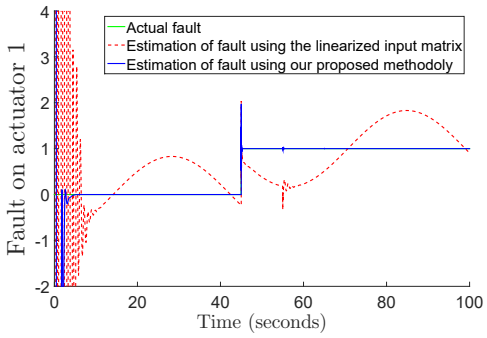

(a) The result for actuator 1.

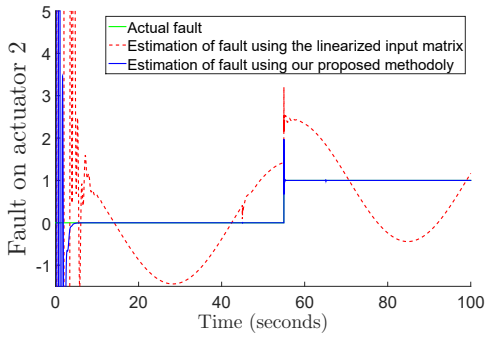

(b) The result for actuator 2.

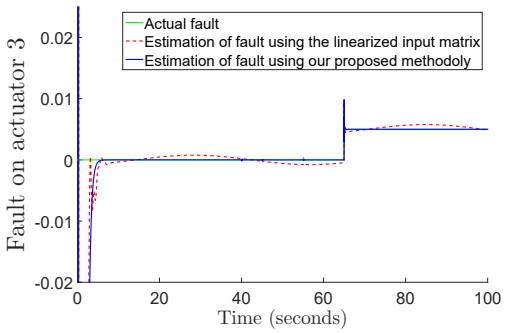

(c) The result for actuator 3.

Figure 3.9: Simulation results for actuator fault estimation using the proposed method vs. those of [60] : the actual and estimated values of $f_a = [1 \quad 1 \quad 0.005]^T$.

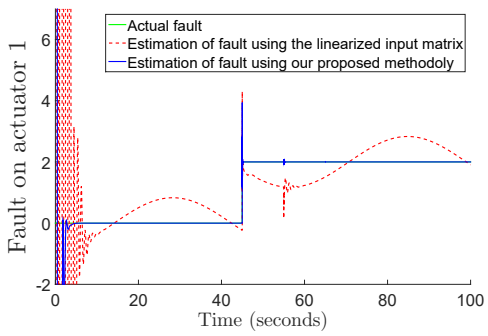

(a) The result for actuator 1.

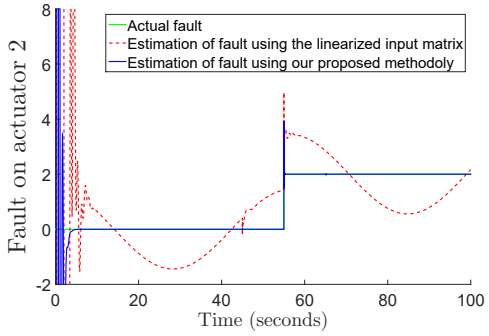

(b) The result for actuator 2.

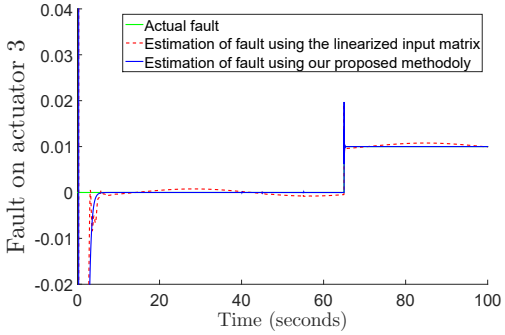

(c) The result for actuator 3.

Figure 3.10: Simulation results for actuator fault estimation using the proposed method vs. those of [60] : the actual and estimated values of $f_a = [2 \quad 2 \quad 0.01]^T$.

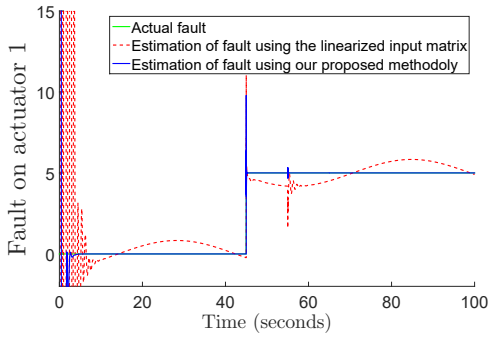

(a) The result for actuator 1.

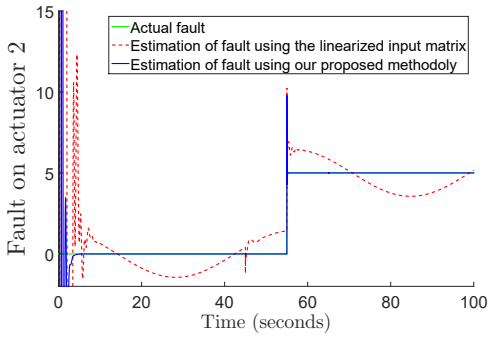

(b) The result for actuator 2.

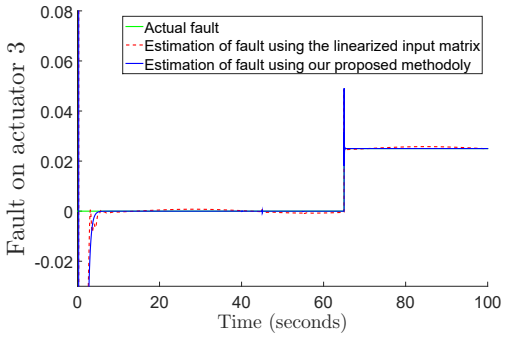

(c) The result for actuator 3.

Figure 3.11: Simulation results for actuator fault estimation using the proposed method vs. those of [60] : the actual and estimated values of $f_a = [5 \quad 5 \quad 0.025]^T$.

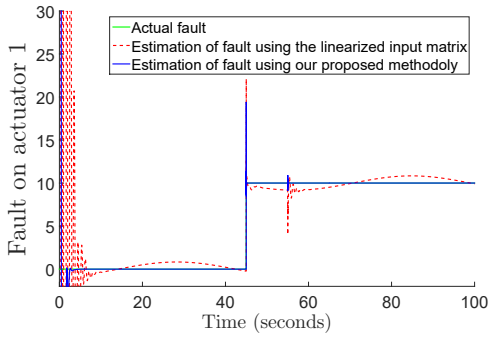

(a) The result for actuator 1.

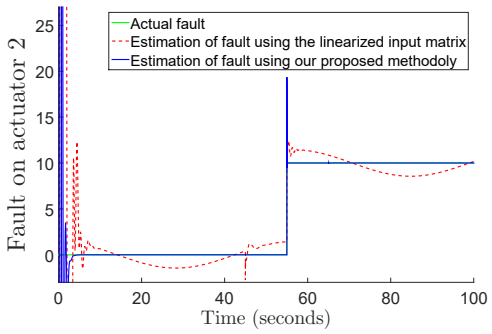

(b) The result for actuator 2.

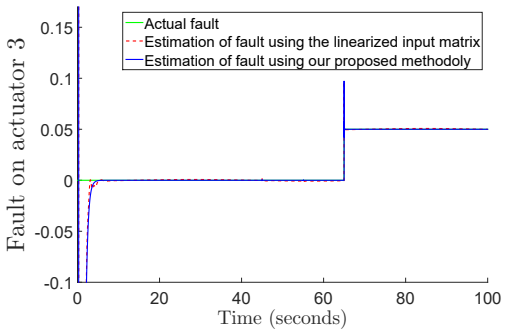

(c) The result for actuator 3.

Figure 3.12: Simulation results for actuator fault estimation using the proposed method vs. those of [60] : the actual and estimated values of $f_a = [10 \quad 10 \quad 0.05]^T$.

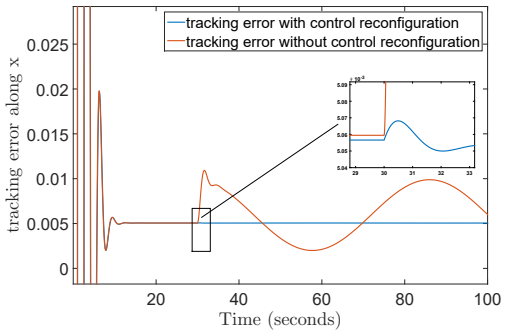

(a) Tracking error along x

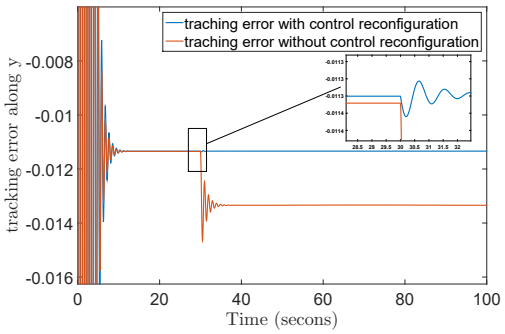

(b) Tracking error along y

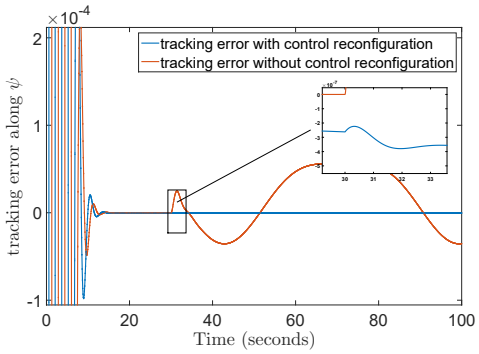

(c) Tracking error along ψ

Figure 3.13: Simulation results using the proposed method for position tracking error with and without fault recovery

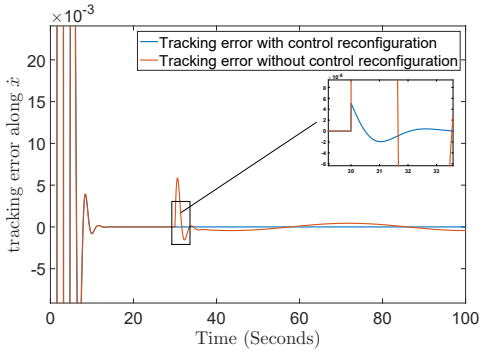

(a) Tracking error along $\dot{x}$

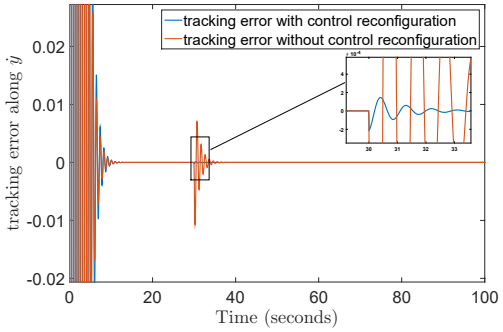

(b) Tracking error along $\dot{y}$

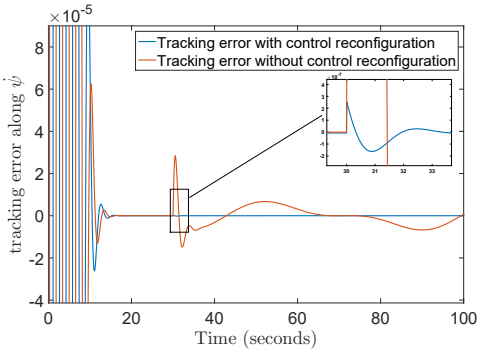

(c) Tracking error along $\dot{\psi}$

Figure 3.14: Simulation results using the proposed method for velocity tracking error with and without fault recovery

3.6 Conclusion

Using the results of Chapter 2, which lead to decoupling the effects of sensor and actuator faults, in this chapter two SMOs have been presented for sensor and actuator fault estimation and reconstruction. The resulting fault estimation has used to reconfigure the controller. Finally, the mathematical proof of stability for the coupled controller, observers and nonlinear plant has been investigated.

Chapter 4

The Proposed Active Fault-Tolerant Control Strategy Using Sliding Mode Controller and Observer

4.1 Introduction

In this chapter, the new methodology for active fault-tolerant scheme is proposed. The methodology presented in this chapter differs from that proposed in Chapter 3 in its fault-tolerant control mechanism. In fact, a SMC approach is used for fault-tolerant control and the SMO observer designed for actuator fault estimation is also omitted. The actuator fault estimation instead can be obtained using the result of the sliding mode

controller. Hence, sliding mode observer is replaced by sliding mode controller which leads in better control performance without compromising fault estimation performance.

The transformation proposed in Chapter 2 is used such that the effect of the sensor and actuator faults are decoupled and the system is divided into two subsystems. However, in this chapter the sliding mode observer is only designed for the first subsystem such that the sensor fault can be estimated using this sliding mode observer. Thereafter, the result of the sensor fault estimation is now fed in to the sliding mode controller. The schematic of the new fault estimation and fault-tolerant control scheme is illustrated in Figure 4.1,

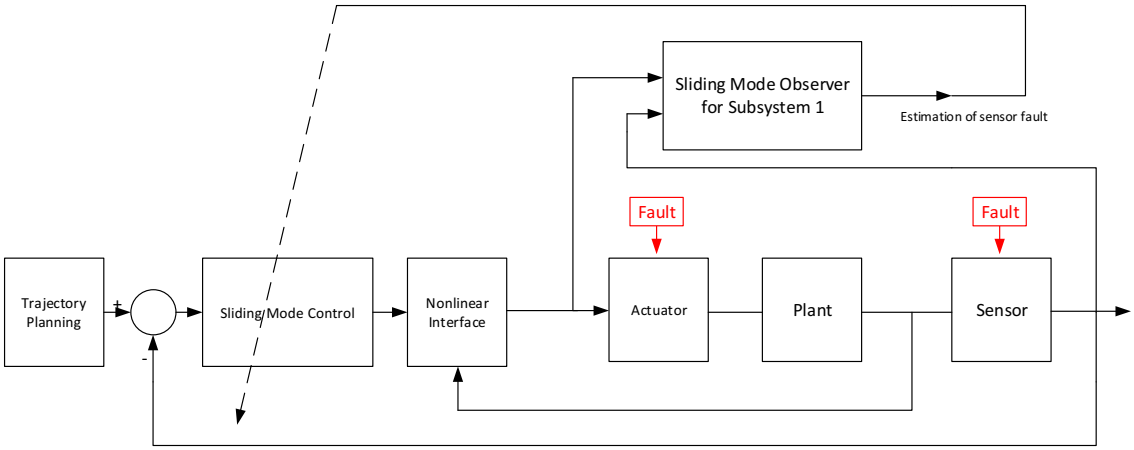

Figure 4.1: The schematic of the proposed active fault tolerant control scheme

The novelty of the FTC approach presented in this chapter as compared to the one

introduced in Chapter 3 is that in this chapter using sliding mode control, **finite time zero tracking error** is guaranteed while using the approach presented in the previous chapter only bounded tracking error is possible.

Moreover, by analyzing the sliding term of the controller, the estimation of the actuator fault is also possible. Therefore, in this chapter, a methodology is proposed using which not only the estimation of the sensor and actuator faults is guaranteed but a better tracking performance is also possible.

This chapter will be presented in the following sequence:

- First, using the results of Chapters 2 and Section 3.2, the transformation and sliding mode observer for Subsystem 1 and hence sensor fault estimation is given.

- Then, the active fault-tolerant control scheme is introduced. In this scheme, the results of the sensor fault estimation is used in the control strategy. Moreover the controller has a sliding term such that it can compensate the effect of the actuator fault in the closed-loop system. Finally, mathematical proof of stability for the pair of robust controller/observer is provided.

- Next, from analyzing the control input signal, the estimation of the actuator fault can be obtained.

- In the final section of this chapter, the simulation results are presented.

4.2 Fault Decoupling and Sensor Fault Estimation

Consider the Euler-Lagrange equations introduced in (1.25)-(1.26). It is shown in Chapter 2 that there exist the state transformation T and output redefinition S such that the original system can be represented as two subsystems such that each subsystem is affected by one type of fault only. Theses transformations have been introduced in (2.4). Moreover, in order to estimate the sensor fault from the first subsystem, a set of exo-state z has been presented such that the sensor fault appears as an unknown input in the state space representation of the system. Thereupon, solving the corresponding LMI feasibility conditions, the transformation T_u were presented for the first subsystem and consequently, the original system is decoupled as shown below.

Subsystem 1:

$$\begin{cases} \dot{q}_1 = A_{q1}q_1 + A_{q2}q_2 + h_2 \\ \dot{q}_2 = A_{q3}q_1 + A_{q4}q_2 + D_{s1}f_s \\ w_3 = q_2 \end{cases}$$

Subsystem 2:

$$\begin{cases} \dot{h}_2 = \bar{f}(T^{-1}h) + \Delta f + g(T^{-1}h)(\tau + f_a) \\ w_2 = C_4 h_2 \end{cases}$$

In this chapter, we design an observer for Subsystem 1 and consequently estimate the sensor fault only. In order to estimate the sensor fault, the sliding mode observer

introduced in Section 3.2 can be used. This observer has been presented in (3.3).

$$\begin{cases} \dot{\hat{q}}_1 = A_{q1}\hat{q}_1 + A_{q2}w_3 + C_4^{-1}w_2 \\ \dot{\hat{q}}_2 = A_{q3}\hat{q}_1 + A_{q4}\hat{q}_2 + L_1(w_3 - \hat{w}_3) + \nu_1 \\ \hat{w}_3 = \hat{q}_2 \end{cases}$$

As presented in Section 3.2, L_1 should be chosen such that $A_{q4} - L_1$ is Hurwitz and ν_1 is governed by (3.6).

$$\nu_1 = \begin{cases} \rho_1 \frac{P_{02}e_{q2}}{\|P_{02}e_{q2}\|}, & \text{if } e_{q2} \neq 0 \\ 0, & \text{otherwise} \end{cases}$$

Using the result of Theorem 3.1, it can be concluded that for any $q(0)$ and $\hat{q}(0)$, there exists ν_1 such that $\hat{q}$ converges to q in finite time.

Consequently, using this observer the sensor fault can be reconstructed with the methodology explained in details in Section 3.3. Therefore, the estimation of the sensor fault can be obtained from (3.18).

$$\hat{f}_s = ((D_{s1})^T D_{s1})^{-1} D_{s1}^T (\rho_1 \frac{P_{02}e_{q2}}{\|P_{02}e_{q2}\| + \delta})$$

In brief, up to this stage, we decoupled the system into two subsystems, each of which is only affected by one type of faults. Then, an observer is designed for Subsystem 1 which is only affected by sensor fault. Therefore, the sensor fault estimation is obtained.

4.3 The Active Fault-Tolerant Control Scheme

Let us consider the state space representation of an Euler-Lagrange system expressed in (3.23).

$$\begin{cases} \dot{x}_1 = x_2 \\ \dot{x}_2 = M^{-1}(x_1)((\tau + f_a) - C_{co}(x_1, x_2)x_2 - G(x_1)) + \Delta f \\ y = Cx + D_s f_s \end{cases}$$

Once more, let us define $H(x_1, x_2) = C_{co}(x_1, x_2)x_2$. Therefore, the system equation can be written as:

$$\begin{cases} \dot{x}_1 = x_2 \\ \dot{x}_2 = M^{-1}(x_1)((\tau + f_a) - H(x_1, x_2) - G(x_1)) + \Delta f \end{cases} \tag{4.3}$$

$$y = Cx + D_s f_s \tag{4.4}$$

Now, consider x_d, $\dot{x}_d$ and $\ddot{x}_d$ as the desired position, velocity an acceleration trajectory, respectively. Hence, for Euler-Lagrange system, the following control input is proposed:

$$\tau = M(\hat{x}_1)aq + H(\hat{x}_1, \hat{x}_2) + G(\hat{x}_1) \tag{4.5a}$$

$$aq = \ddot{x}_d(t)K_0(\hat{x}_1 x_d(t))K_1(\hat{x}_2 - \dot{x}_d(t)) - \nu_2 \tag{4.5b}$$

where

$$\nu_2 = \begin{cases} \rho_2 \frac{v}{\|v\|}, & \text{if } v \neq 0 \\ 0, & \text{otherwise} \end{cases} \tag{4.6}$$

and $\hat{x} = C^{-1}(y - D_s \hat{f}_s)$. Moreover, $\hat{f}_s$ is the estimation of the sensor fault coming from the sliding mode observer. Further, K_0 and K_1 are positive diagonal matrices corresponding to position and velocity gains. The control signal v and the corresponding weight ρ_2 in sliding term ν_2 will be defined later throughout the proof of the following theorem which constitutes the main result of this chapter.

Theorem 4.1. *Consider the closed-loop system illustrated in Figure 4.1, where the plant is an EL system modeled by (3.23) affected by simultaneous sensor and actuator faults, the observer is given in (3.3), the control input is given in (4.5) and (4.6). Then, under Assumptions 1 and 2, the proposed fault-tolerant control scheme can maintain the closed-loop system stability in the presence of simultaneous sensor and actuator faults.*

Proof. The outline of the proof is stated first:

- Step 1: Given sensor fault estimation structure (3.18), we show that the estimates of sensor faults are bounded.

- Step 2: Considering the properties of EL systems, we show that the closed-loop error dynamics can be expressed as linear dynamics subject to the terms bounded by position and velocity tracking errors.

- Step 3: Design the sliding term ν_2 (see (4.6)) in terms of nonfaulty part of the measurement only.

- Step 4: The closed-loop system stability can be inferred by Lyapunov's direct method.

- Step 5: Using the results of Theorem 3.1, the convergence of estimated sensor faults to their respective true values is concluded in **finite time**.

In sequel, the details of the proof is presented:

• Step 1: The boundedness of the sensor fault estimation is clear from (3.18), as also discussed in Chapter 3.

• Step 2: First, substitute the control input (4.5a) into system equation (3.23):

$$\begin{cases} \dot{x}_1 = x_2 & \text{(4.7a)} \\ \dot{x}_2 = M^{-1}(x_1)((H(\hat{x}_1,\hat{x}_2) - H(x_1,x_2)) + (G(\hat{x}_1) - G(x_1)) + & \text{(4.7b)} \\ \qquad M(\hat{x}_1)aq + f_a) + \Delta f \end{cases}$$

Multiplying both sides of (4.7b) by $M(x_1)$ yields in:

$$\begin{aligned} M(x_1)\dot{x}_2 \quad = \quad & (H(\hat{x}_1,\hat{x}_2) - H(x_1,x_2)) + (G(\hat{x}_1) - G(x_1)) + \\ & M(\hat{x}_1)aq + f_a + M(x_1)\Delta f \end{aligned} \tag{4.8}$$

Now, by adding and subtracting $M(\hat{x}_1)\dot{x}_2$ to the right hand side of (4.8), we will get:

$$M(\hat{x}_1)(\dot{x}_2 - aq) = (H(\hat{x}_1, \hat{x}_2) - H(x_1, x_2)) + (G(\hat{x}_1) - G(x_1)) + (M(\hat{x}_1) - M(x_1))\dot{x}_2 + f_a + M(x_1)\Delta f \quad (4.9)$$

Then, by substituting aq from (4.5b) into (4.9) we will obtain:

$$\ddot{\tilde{x}} + K_1\dot{\tilde{x}} + K_0\tilde{x} = F + M^{-1}(\hat{x}_1)f_a - \nu_2 \quad (4.10)$$

where $\ddot{\tilde{x}} = \dot{x}_2 - \ddot{x}_d$, $\dot{\tilde{x}} = x_2 - \dot{x}_d$ and $\tilde{x} = x_1 - x_d$. Moreover we have:

$$F = M^{-1}(\hat{x}_1)((H(\hat{x}_1, \hat{x}_2) - H(x_1, x_2)) + (G(\hat{x}_1) - G(x_1)) + (M(\hat{x}_1) - M(x_1))\dot{x}_2 + M(x_1)\Delta f) + (K_1\Delta x_2 + K_0\Delta x_1) \quad (4.11)$$

In (4.11), Δx_1 and Δx_2 are the terms appear due to the sensor fault estimation error:

$$\begin{aligned} \Delta x &= \hat{x} - x \\ &= C^{-1}(y - D_s\hat{f}_s) - C^{-1}(y - D_s f_s) \\ &= C^{-1}D_s(\hat{f}_s - f_s) \end{aligned} \quad (4.12)$$

As discussed in details in Chapter 3, since f_s is bounded based on Assumption 2 and $\hat{f}_s$ is bounded based on (3.18), we can conclude that Δx defined in (4.12) is bounded

as well.

Defining the tracking error vector as $e_t^T = [\dot{\tilde{x}}^T \quad \tilde{x}^T]$, we have:

$$\dot{e}_t = A_t e_t + \begin{bmatrix} 0 \\ F + M^{-1}(\hat{x}_1) f_a - \nu_2 \end{bmatrix} \tag{4.13}$$

where K_0 and K_1 are chosen such that $A_t = \begin{bmatrix} 0 & I \\ -K_0 & -K_1 \end{bmatrix}$ is Hurwitz.

In addition, as mentioned before ν_2 is the sliding term. In order to guarantee the stability of the closed-loop system using the sliding mode controller, the knowledge of the upper bound of the terms F and f_a are required. Towards this end, let us investigate the terms in F given in (4.11). Following similar analysis and discussion given in Chapter 3 we have:

$$\|H(\hat{x}_1, \hat{x}_2) - H(x_1, x_2)\| < \gamma_{11} + \gamma_{21}\|\tilde{x}\| + \gamma_{31}\|\dot{\tilde{x}}\| + \gamma_4\|\dot{\tilde{x}}\|^2 \tag{4.14}$$

$$\|(G(\hat{x}_1) - G(x_1))\| < \gamma_{12} \tag{4.15}$$

$$\|(M(\hat{x}_1) - M(x_1))\dot{x}_2\| < \gamma_{32}\|\dot{\tilde{x}}\| \tag{4.16}$$

$$\|M(x_1)\Delta f\| < \gamma_{13} \tag{4.17}$$

$$\|M(\hat{x}_1)(K_1\Delta x_2 + K_0\Delta x_1)\| < \gamma_{14} \tag{4.18}$$

$$\|M^{-1}(\hat{x}_1) f_a\| < \gamma_{15} \tag{4.19}$$

Hence, in overall we can conclude that, there exist positive scalar α_1, α_2 and α_3

such that:

$$\|F + M^{-1}(\hat{x}_1)f_a\| \quad < \quad \alpha_1 + \alpha_2\|e_t\| + \alpha_3\|e_t\|^2 \tag{4.20}$$

On the other hand, by defining $B = \begin{bmatrix} 0_m \\ I_m \end{bmatrix}$, we can restate (4.13) as follows:

$$\dot{e}_t \quad = \quad A_t e_t + B(F + M^{-1}(\hat{x}_1)f_a - \nu_2) \tag{4.21}$$

Now, let us multiply both sides of (4.13) by the transformation T introduced in (2.4). As discussed in Chapter 2, the transformation T is introduced to decouple the effect of the sensor and actuator faults. Hence, by introducing $e_h^T = [e_{h1}^T \quad e_{h2}^T]$ where $e_h = Te_t$, the tracking error dynamics in the transformed representation will be given by:

$$\dot{e}_h \quad = \quad TA_tT^{-1}e_h + B(F + M^{-1}(\hat{x}_1)f_a - \nu_2) \tag{4.22}$$

- Step 3: To proceed further, we first state the following Kalman-Yakubovich Lemma.

Lemma 4.1. (Kalman-Yakubovich-Popov Lemma) *Let $Z(s) = C(sI - A)^{-1}B + D$ be a $p \times p$ transfer function matrix, where A is Hurwitz, (A, B) is controllable, and (A, C) is observable. Then, $Z(s)$ is strictly positive real if and only if there exist a positive definite symmetric matrix P, matrices W and L and a positive constant ε such*

that:

$$PA + A^T P = -L^T L - \varepsilon P \tag{4.23}$$

$$PB = C^T - L^T W \tag{4.24}$$

$$W^T W = D + D^T \tag{4.25}$$

Our objective is to design the robustifying term ν_2 in terms of e_{h2} only (the error corresponding to Subsystem 2 (see (2.13) and (2.14))), since e_{h1} is contaminated by sensor faults. Hence, we define $C_h = [0_m, C_4]$.

Now, since T is a similarity transformation, $A_h = TA_tT^{-1}$ is Hurwitz as well. Moreover, given the fact that the state feedback does not change the controllability, the pair (A_t, B) is controllable. Furthermore, considering the format of the transformation T in (2.11), it is clear that $TB = B$. Note that, controllability is also invariant under similarity transformation T. Hence, we can conclude that the pair (A_h, B) is also controllable. On the other hand, the observability of the fully actuated EL system is guaranteed from either full position or full velocity measurement or any full rank combination of them. Hence, given the full rank condition on C_4, we can infer the observability of the pair (A_h, C_h).

Given that A_h is Hurwitz, (A_h, B) is controllable, and (A_h, C_h) is observable we can apply the above Kalman-Yakubovich-Popov (KYP) lemma to our EL system, i.e. for given $Q = Q^T > 0$, we can find positive definite matrix P such that:

$$A_h^T P + P A_h = -Q \tag{4.26}$$

$$PB = C_h^T \tag{4.27}$$

Note that, the structure of B and C_h^T reveals that each element of the underlying transfer matrix possesses relative degree one. Since, A_h is Hurwitz, by proper selection of K_0, K_1, T and S the SPR condition required for KYP lemma can be satisfied.

• Step 4: Now, consider the following Lyapunov function:

$$V = e_h^T P e_h \tag{4.28}$$

where P is positive definite matrix with proper dimension satisfying (4.26) and (4.27). The derivative of the Lyapunov function candidate along the trajectory of the system (4.22) is given by:

$$\dot{V} = -e_h^T Q e_h + 2 e_h^T P B (F + M^{-1}(\hat{x}_1) f_a - \nu_2) \tag{4.29}$$

Then, by invoking KYP Lemma ($PB = C_h^T$), one can get:

$$\dot{V} = -e_h^T Q e_h + 2 e_h^T C_h^T (F + M^{-1}(\hat{x}_1) f_a - \nu_2) \tag{4.30}$$

$$= -e_h^T Q e_h + 2 (C_4 e_{h2})^T (F + M^{-1}(\hat{x}_1) f_a - \nu_2) \tag{4.31}$$

Thereupon, in the sliding term expressed in (4.6), we define:

$$\rho_2(e_t, t) > \alpha_1 + \alpha_2\|e_t\| + \alpha_3\|e_t\|^2 \tag{4.32}$$

$$v = C_4 e_{h2} \tag{4.33}$$

Therefore, by substituting the sliding term ν_2 from (4.6) into (4.31) we have:

$$\dot{V} = -e_h^T Q e_h + 2v^T(F + M^{-1}(\hat{x}_1)f_a - \rho_2(e_{h1}, t)\frac{v}{\|v\|}) \tag{4.34}$$

Using the Cauchy-Schwartz inequality, the second term of (4.34) can be expressed as:

$$\begin{aligned} 2v^T(F + M^{-1}(\hat{x}_1)f_a - \rho_2(e_t, t)\frac{v}{\|v\|}) &\leq -\rho_2(e_t, t)\|v\| + \|v\|(F + M^{-1}(\hat{x}_1)f_a) \\ &= \|v\|(F + M^{-1}(\hat{x}_1)f_a - \rho_2(e_t, t)) \end{aligned} \tag{4.35}$$

Since $\|F + M^{-1}(\hat{x}_1)f_a\| < \|\rho_2\|$, we can get:

$$\dot{V} \leq -e_h^T Q e_h \tag{4.36}$$

We can conclude that e_h and hence e_t converge to zero. The convergence of e_t results in the boundedness of $\tilde{x}$ and $\dot{\tilde{x}}$ which in turn leads us to the boundedness of the system states, i.e. $x_1 \quad and \quad x_2 \in L_\infty$.

• Step 5: Given the boundedness of the system states, stability and convergence

of SMO are guaranteed based on the result of Theorem 3.1. Hence the sensor fault estimate $\hat{f}_s$ converges to its true value in **finite time**. □

Moreover, in steady state when observation and the tracking error converge to zero, (4.10) can be expressed as:

$$0 = \Delta f + M^{-1}(\hat{x}_1) f_a - \nu_2 \tag{4.37}$$

Hence, the estimate of the actuator fault can be obtained from:

$$\hat{f}_a = M(\hat{x}_1)^{-1}(\nu_{eq2} - \Delta\bar{f}) \tag{4.38}$$

where ν_{eq2} is the sigmoid function approximation of ν_2. Then, we can write the estimate of f_a according to:

$$\hat{f}_a = M(\hat{x}_1)^{-1}(\rho_2 \frac{v}{\|v\|+\delta} - \Delta\bar{f}) \tag{4.39}$$

Note that in (4.39), $\Delta\bar{f}$ represents the upper bound of the uncertainties, unmodeled dynamics and disturbances in the EL system. We should emphasize that in the presence of large uncertainties and disturbances, even though the estimation accuracy decreases, nevertheless the closed-loop system would still maintain the overall stability and tracking property.

4.4 Simulation Results

To evaluate the performance of our proposed fault accommodation and estimation strategy, a set of simulations are performed below on the autonomous underwater vehicle (AUV) modeled by EL equations as in (1.23). The numerical values of the parameters are given in (3.49) to (3.51). Moreover, with the same model, we will have the same transformations given in (3.52) to (3.57). In simulations conducted below, the sensor faults, their distribution matrices, actuator fault and the ocean current model are the same scenario given in (3.59) to (1.20).

The fault estimation results are illustrated in Figures 4.2 and 4.3. The results given in these figures illustrate that the sensor and actuator faults are successfully estimated by our proposed method. As can be seen, the estimated faults show an error of zero during the fault free interval (i.e., $t \leq 40$ in Fig. 3.3 and $t \leq 45$ in Fig. 3.4). On the event that the faults starts to build up, the estimator promptly reacts and estimate the true value of the fault with a reasonable settling time.

However, it should be noted that, the fault estimation results will be affected by the measurement noise, modeling uncertainties and disturbances. Therefore, to evaluate the performance of the proposed fault detection and isolation strategy, a Monte Carlo simulation was performed. We have run the simulation for 30 times. The uncertainty and disturbances used in the simulation are modeled by Δf in dynamic model (1.25).

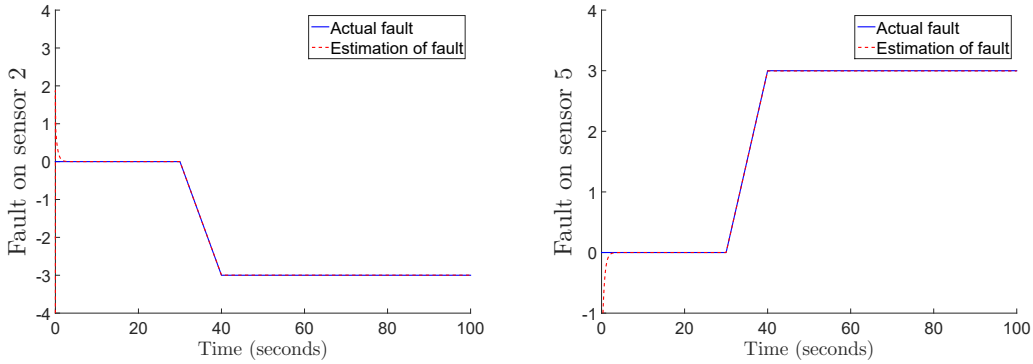

(a) The result for position sensor 2.

(b) The result for velocity sensor 2.

Figure 4.2: Simulation results for sensor fault estimation: the actual and estimated values of f_s.

In Monte Carlo simulations, the disturbance for the AUV is considered as the ocean current, the details of which are given at (1.20). Moreover, the measurement noise is considered as a band-limited white noise with normal distribution and power (height of power spectral density) of 0.01. The results are represented graphically as shown in Figures 4.4 and 4.5.

Monte Carlo simulation can be used to obtain a proper threshold level based on the property of the noise and uncertainty in the system. The suggested threshold level for each channel is given in Table 4.1. We can see that the threshold for each fault in each channel is different. Based on the Monte Carlo simulation results, any actuator fault greater the defined threshold value in the table is detectable.

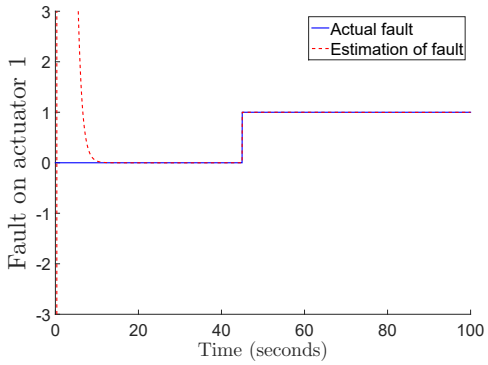

(a) The result for actuator 1.

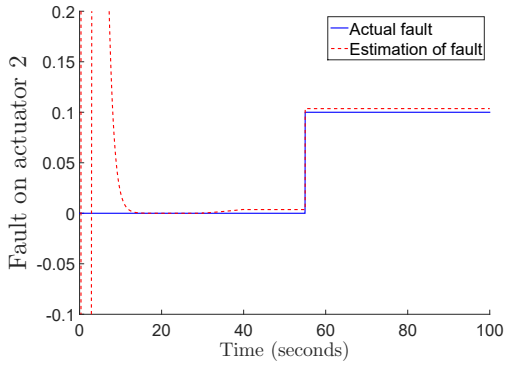

(b) The result for actuator 2.

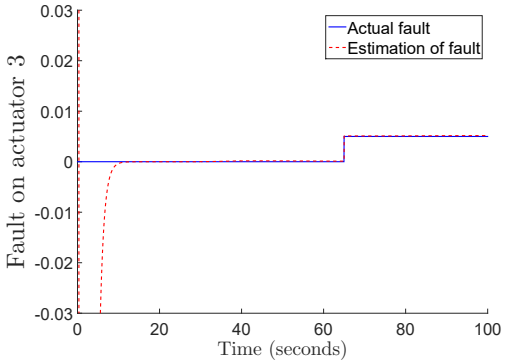

(c) The result for actuator 3.

Figure 4.3: Simulation results for actuator fault estimation: the actual and estimated values of f_a.

f_{a1}	f_{a2}	f_{a3}	f_{s1}	f_{s2}
0.17	0.35	0.0004	0.12	0.13

Table 4.1: Fault detection thresholds found using Monte Carlo simulations

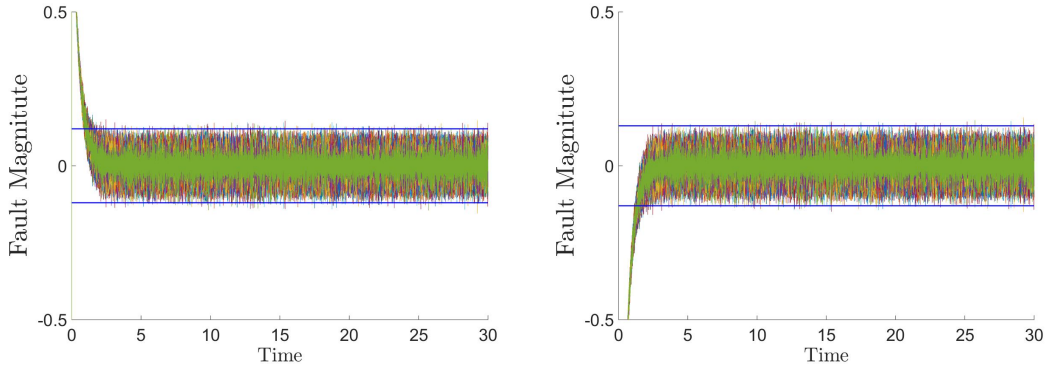

(a) The result for position sensor 2.

(b) The result for velocity sensor 2.

Figure 4.4: The result of Monte Carlo simulations performed for proper threshold setting for sensor fault estimation.

Moreover, in Figure 4.6 and 4.7 the simulation results in the presence of measurement noise are given. In the simulation, the output measurement was contaminated by white noise with the property given before.

Figure 4.6 shows that the sensor fault estimation is still possible by employing our proposed methodology in the presence of measurement noise. Similarly, the actuator fault estimation in the presence of measurement noise is also depicted in Figure 4.7. It can be seen that the actuator fault is also estimated successfully.

Furthermore, the results of fault-tolerant control scheme are illustrated in Figure 4.8 to 4.9. From these figures, we can see that in the presence of faults, zero steady state error is obtainable using the proposed fault accommodation strategy. As shown in the figures, a smooth and fairly fast convergence is exhibited.

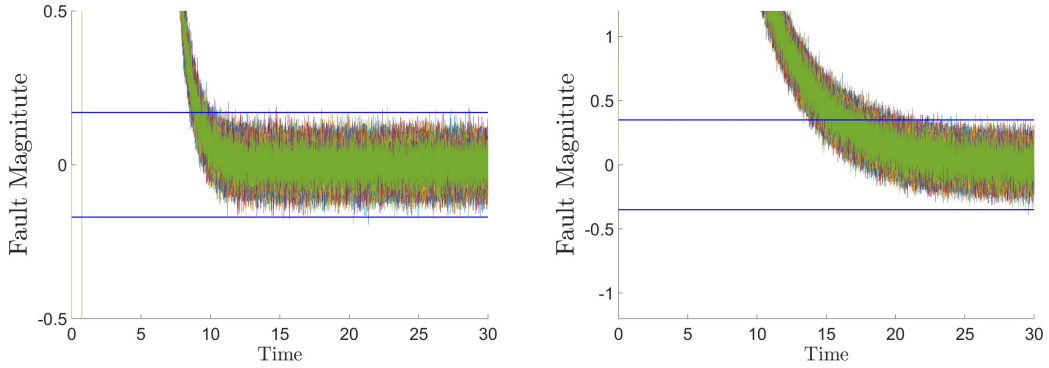

(a) The result for actuator 1.

(b) The result for actuator 2.

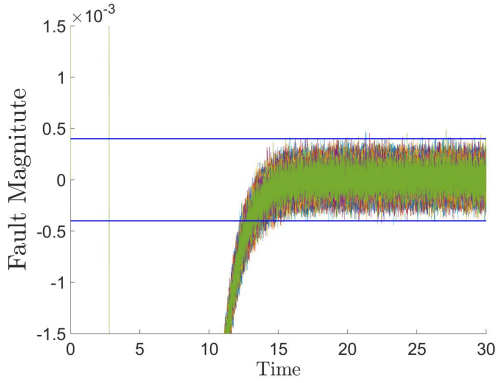

(c) The result for actuator 3.

Figure 4.5: The result of Monte Carlo simulations performed for proper threshold setting for actuator fault estimation.

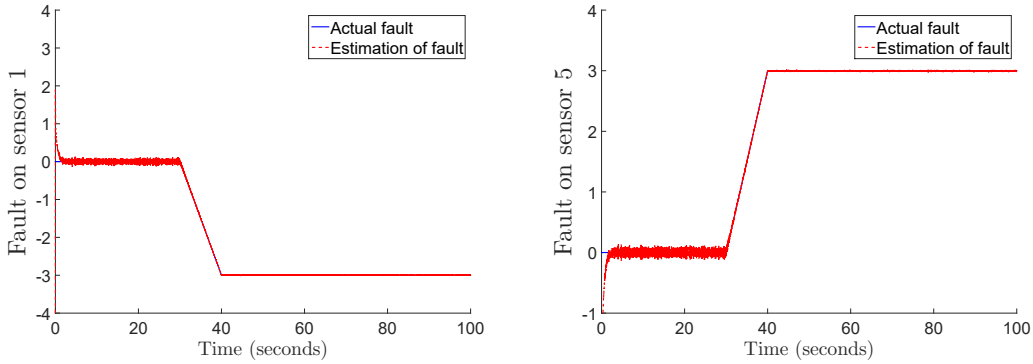

(a) The result for position sensor 2.

(b) The result for velocity sensor 2.

Figure 4.6: Simulation results for sensor fault estimation in the presence of measurement noises: the actual and estimated values of f_s.

To evaluate the performance of the fault-tolerant control strategies proposed in this thesis, a comparative simulation has been performed. In Chapter 3 a fault-tolerant control strategy (FTC1) based on both sensor and actuator fault reconstruction has been presented. Simulation results showed a good performance in the presence of noises and disturbances with fairly moderate magnitude. The aim of the following simulation study is to compare the performance of FTC1 to that of the fault-tolerant control strategy presented in this chapter (FTC2) which is based on sensor fault reconstruction and sliding mode controller, in the presence of large disturbances. The following scenario is considered for the final set of simulations:

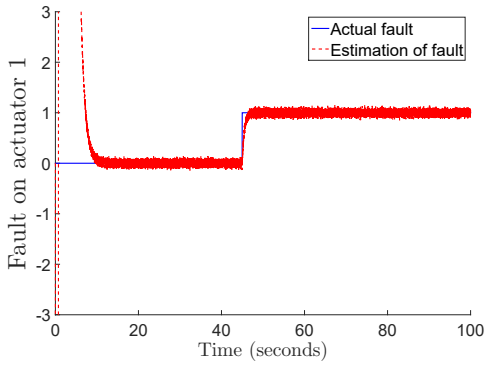

(a) The result for actuator 1.

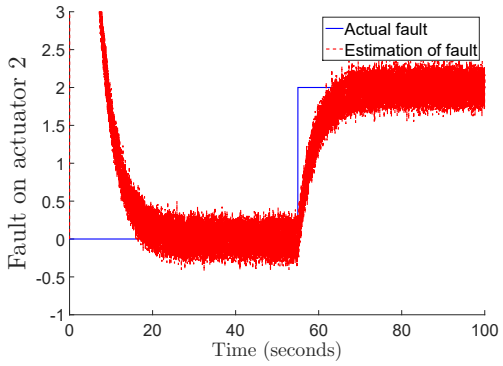

(b) The result for actuator 2.

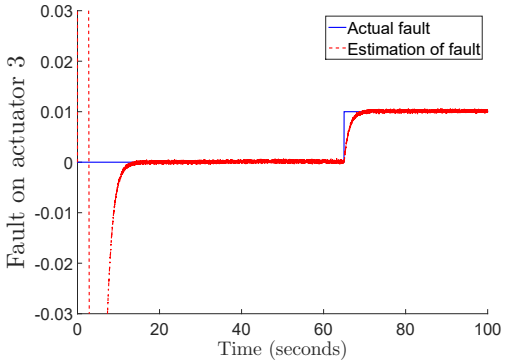

(c) The result for actuator 3.

Figure 4.7: Simulation results for actuator fault estimation in the presence of measurement noises: the actual and estimated values of f_a.

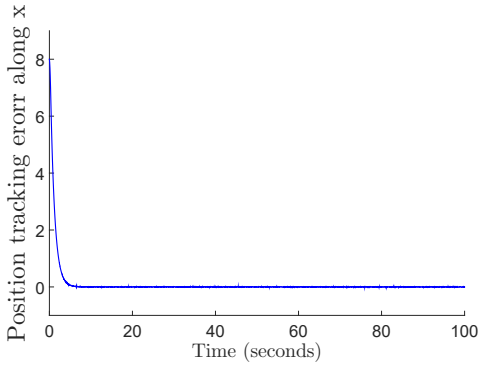

(a) Tracking error along x

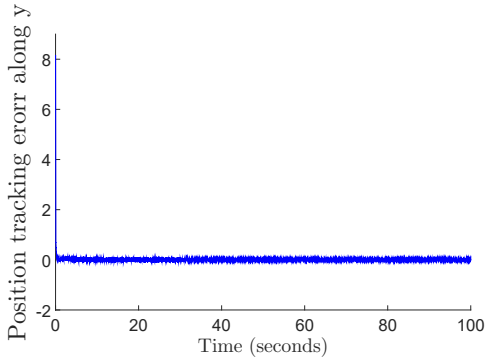

(b) Tracking error along y

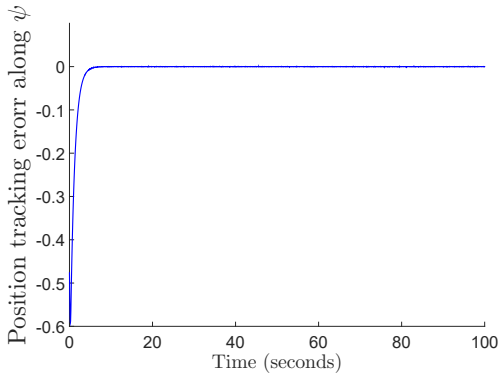

(c) Tracking error along ψ

Figure 4.8: Simulation results using robust FTC approach for position tracking error

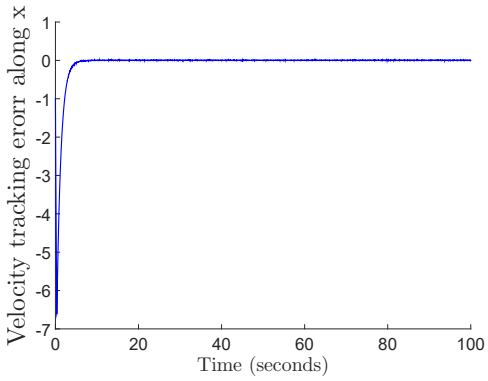

(a) Tracking error along $\dot{x}$

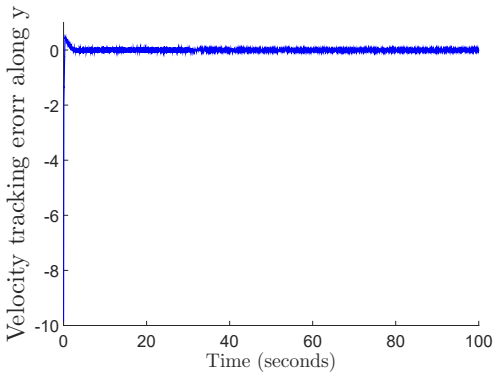

(b) Tracking error along $\dot{y}$

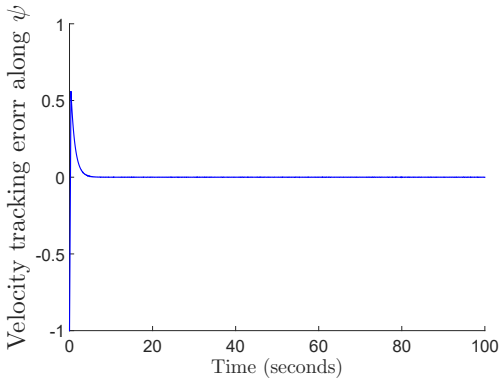

(c) Tracking error along $\dot{\psi}$

Figure 4.9: Simulation results using robust FTC approach for velocity tracking error

$$X_d = \begin{bmatrix} 9\cos(t) \\ t/3 \\ 1 \end{bmatrix} \tag{4.40}$$

$$K_0 = I_3 \tag{4.41}$$

$$K_1 = I_3 \tag{4.42}$$

$$dc(0) = [4, 10, 0]^T \tag{4.43}$$

The rest of the parameters including fault signals are the same of those given in Section 3.5. The results of fault estimations are shown in Figure 4.12 to 4.13 for FTC1 and FTC2, respectively. As can be seen, sensor fault estimation is intact whereas the result of actuator fault estimation is deteriorated due to the presence of large disturbances.

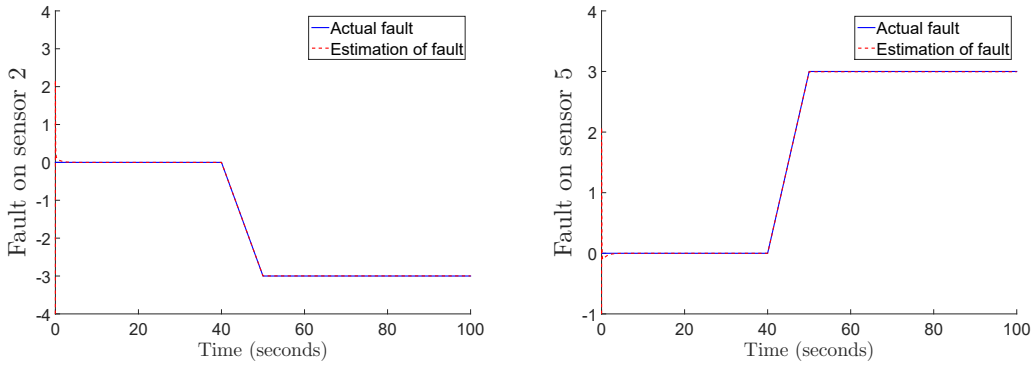

(a) The result for position sensor 2.

(b) The result for velocity sensor 2.

Figure 4.10: Simulation results for sensor fault estimation using FTC1 in the presence of large disturbances: the actual and estimated values of f_s.

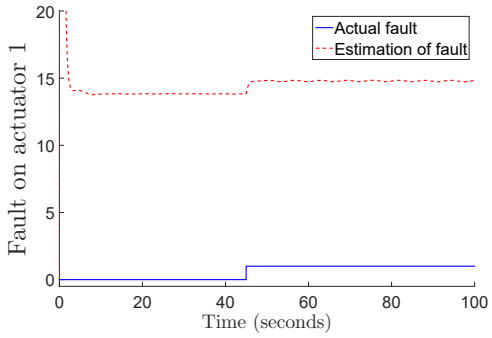

(a) The result for actuator 1.

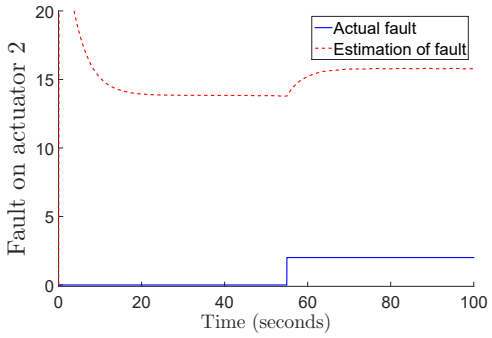

(b) The result for actuator 2.

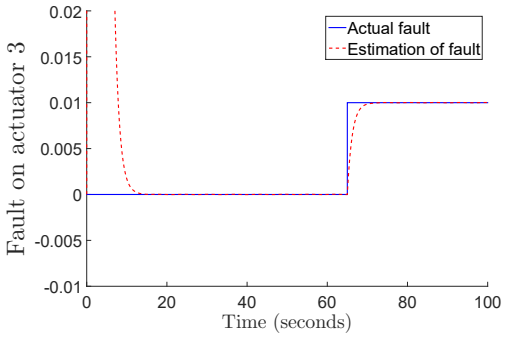

(c) The result for actuator 3.

Figure 4.11: Simulation results for actuator fault estimation using FTC1 in the presence of large disturbances: the actual and estimated values of f_a.

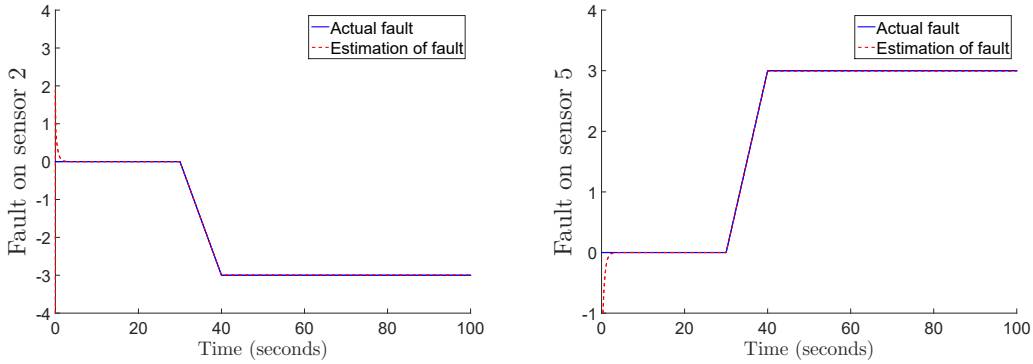

(a) The result for position sensor 2.

(b) The result for velocity sensor 2.

Figure 4.12: Simulation results for sensor fault estimation using FTC2 in the presence of large disturbances: the actual and estimated values of f_s.

Since reconfiguration scheme in FTC1 is based on fault estimations, any actuator fault estimation error directly results in a poor tracking performance. However, the fault-tolerant control strategy presented in this chapter (FTC2) is based on a robust SMC in which the actuator fault estimation error is accounted for. Figure 4.14 and 4.15 illustrate the tracking error for both fault-tolerant schemes. It can be observed that the results obtained by using FTC2 are superior than those obtained by using FTC1.

4.5 Conclusion

Using the same decoupling methodology presented in Chapter 2, a robust fault-tolerant control scheme has been introduced in this chapter based on sliding mode controller. In

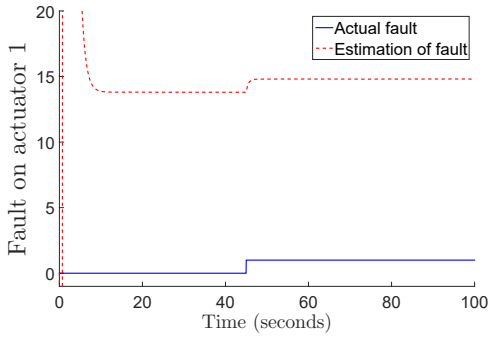

(a) The result for actuator 1.

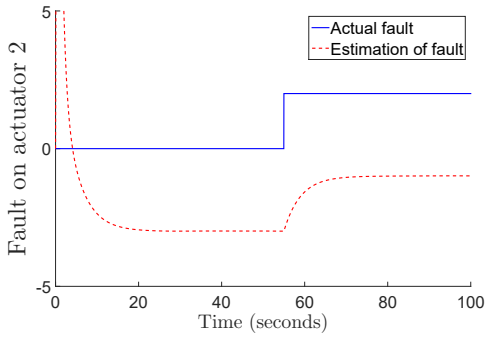

(b) The result for actuator 2.

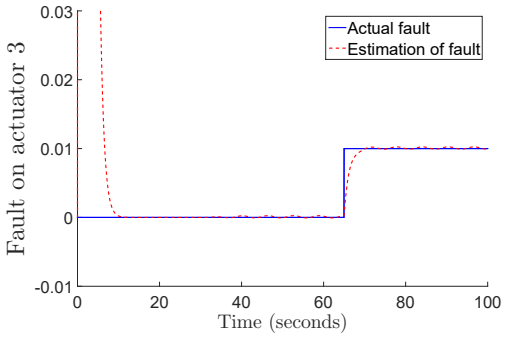

(c) The result for actuator 3.

Figure 4.13: Simulation results for actuator fault estimation using FTC2 in the presence of large disturbances: the actual and estimated values of f_a.

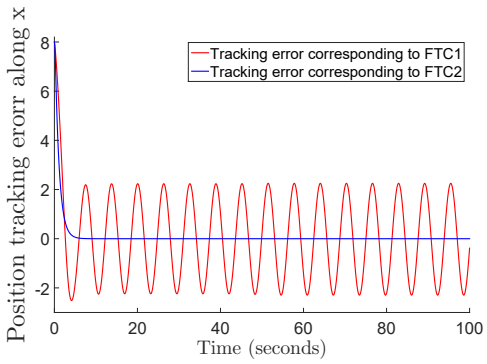

(a) Tracking error along x

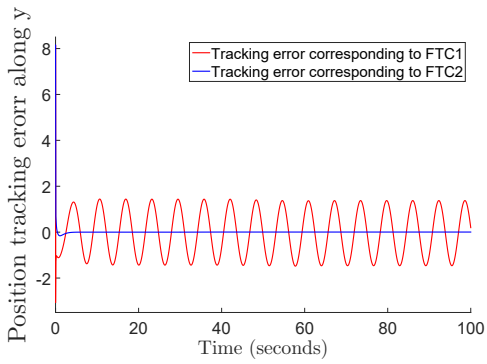

(b) Tracking error along y

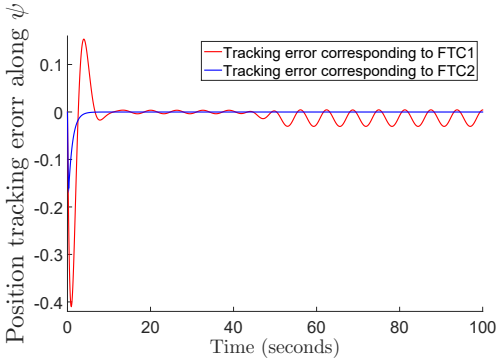

(c) Tracking error along ψ

Figure 4.14: Simulation results for position tracking error using FTC1 vs. FTC2

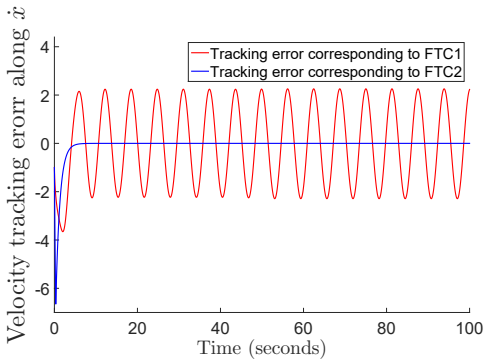

(a) Tracking error along $\dot{x}$

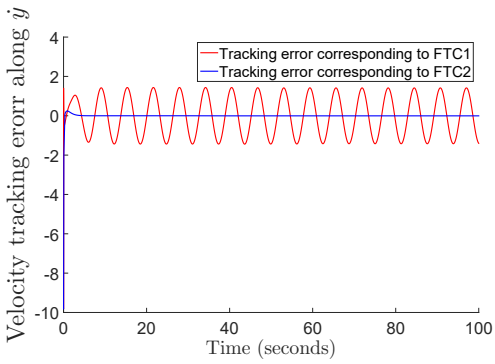

(b) Tracking error along $\dot{y}$

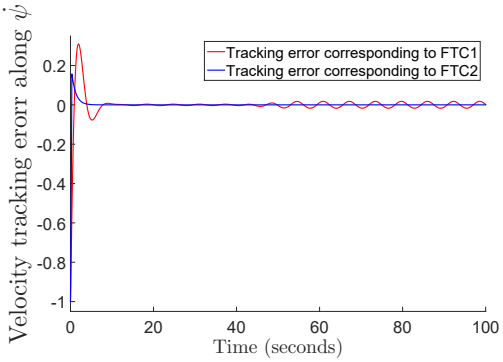

(c) Tracking error along $\dot{\psi}$

Figure 4.15: Simulation results for velocity tracking error using FTC1 vs. FTC2

this approach, only the sensor fault estimation is fed back to the controller in order to correct the faulty measurement. However to deal with actuator faults, a robust sliding mode controller has been used. As a result, the tracking performance is preserved in the presence of actuator faults. Finally, the actuator faults have been reconstructed by using the controller sliding surface.

Chapter 5

Conclusions and Future Work

This chapter concludes the thesis and provides some suggestions for further research.

5.1 Conclusions

In this thesis, the problem of fault estimation and accommodation for Euler-Lagrange systems subject to sensor and actuator faults has been addressed.

Towards this end, first an output redefinition and state transformation have been introduced such that the effects of the sensor and actuator faults are decoupled. Using these transformations, the system was decomposed into two subsystems, such that the first subsystem affected by sensor faults and second subsystem affected by actuator faults only. Consequently, a procedure based on two LMI feasibility conditions has been proposed to find such transformations. The result of this fault decoupling transformation

has been used in subsequent chapters to develop two novel FDIE and FTC strategies.

In the first scheme, two sliding mode observers have been used to reconstruct the sensor and actuator faults, separately, the result of which are fed back to the controller to compensate the effect of faults. The mathematical proof of stability for coupled controller, observers and nonlinear plant has been demonstrated as well. Simulation results performed on a 3DOF AUV modeled with EL equations were presented to demonstrate the effectiveness of the proposed FDIE and FTC methodologies.

In the second scheme, the same decoupling transformations have been used. However, sliding mode observer was utilized for sensor fault only. The results of sensor fault reconstruction have been employed to reconfigure the controller and rectify the effect of sensor faults. However, to deal with actuator faults, a robust sliding mode controller is used, as a result of which zero tracking convergence and actuator fault estimation are possible. The stability proof as well as a comparative study performed on the same AUV model have been presented to evaluate the performance of the two proposed methodologies.

5.2 Future Work

In this work, it was assumed that a full-state measurement is available. However, the presented transformations can be still applied under output measurements, provided that underlying assumptions are satisfied. We have proposed an analytical procedure

using LMI technique to find these transformations for the case of full state measurement. Hence, an analytical procedure similar to that proposed in this thesis can be sought to find such transformations for general output feedback scenario. In this case, it should be noted that reducing the number of measurement will reduce the sensor and equipment expenses, however the number of detectable faults will be limited as well. Thereupon, if the transformation can be obtained for this case, a new output feedback fault tolerant control strategy can also be considered in future as the extension to this study.

Moreover, after decoupling the effect of sensor and actuator faults using the coordinate and output transformations, other types of observers or estimation techniques such as adaptive approaches or unknown input observer techniques can be applied as well. Further, other fault tolerant control schemes for closed-loop system may be required, since the observer and controller are coupled in this nonlinear system.

In this research, fault estimation and fault tolerant control strategy are designed for nonlinear systems governed by Euler-Lagrange equations. The study of using the proposed transformations, fault estimation and/or fault tolerant control for broader classes of nonlinear systems subject to simultaneous sensor and actuator fault may be an interesting topic for future research.

Bibliography

[1] R. Isermann, *Fault-diagnosis systems: an introduction from fault detection to fault tolerance*. Springer Science & Business Media, 2006.

[2] S. Allen and A. Caglayan, "An expert system approach to global fault detection and isolation design," CHARLES RIVER ANALYTICS INC CAMBRIDGE MA, Tech. Rep., 1990.

[3] N. J. Scenna, "Some aspects of fault diagnosis in batch processes," *Reliability Engineering & System Safety*, vol. 70, no. 1, pp. 95–110, 2000.

[4] R. J. Patton, P. M. Frank, and R. N. Clark, *Issues of fault diagnosis for dynamic systems*. Springer Science & Business Media, 2013.

[5] M. Ahmed, M. Geliel, and A. Khalil, "Power transformer fault diagnosis using fuzzy logic technique based on dissolved gas analysis," in *Control & Automation (MED), 2013 21st Mediterranean Conference on*. IEEE, 2013, pp. 584–589.

[6] H. A. Talebi, K. Khorasani, and S. Tafazoli, "A recurrent neural-network-based sensor and actuator fault detection and isolation for nonlinear systems with application to the satellite's attitude control subsystem," *IEEE Transactions on Neural Networks*, vol. 20, no. 1, pp. 45–60, 2009.

[7] T. Sorsa and H. N. Koivo, "Application of artificial neural networks in process fault diagnosis," *Automatica*, vol. 29, no. 4, pp. 843–849, 1993.

[8] X. Ding, L. Guo, and T. Jeinsch, "A characterization of parity space and its application to robust fault detection," *IEEE Transactions on Automatic Control*, vol. 44, no. 2, pp. 337–343, 1999.

[9] E. Chow and A. Willsky, "Analytical redundancy and the design of robust failure detection systems," *IEEE Transactions on automatic control*, vol. 29, no. 7, pp. 603–614, 1984.

[10] M. Soroush, "State and parameter estimations and their applications in process control," *Computers & Chemical Engineering*, vol. 23, no. 2, pp. 229–245, 1998.

[11] T. Jiang, K. Khorasani, and S. Tafazoli, "Parameter estimation-based fault detection, isolation and recovery for nonlinear satellite models," *IEEE Transactions on control systems technology*, vol. 16, no. 4, pp. 799–808, 2008.

[12] B. Jiang and F. Chowdhury, "Observer-based fault diagnosis for a class of nonlinear systems," in *American Control Conference, 2004. Proceedings of the 2004*, vol. 6. IEEE, 2004, pp. 5671–5675.

[13] G.-R. Duan and R. J. Patton, "Robust fault detection using luenberger-type unknown input observers-a parametric approach," *International Journal of Systems Science*, vol. 32, no. 4, pp. 533–540, 2001.

[14] J. Chen, R. J. Patton, and H.-Y. Zhang, "Design of unknown input observers and robust fault detection filters," *International Journal of control*, vol. 63, no. 1, pp. 85–105, 1996.

[15] J. Zhang, A. K. Swain, and S. K. Nguang, *Robust Observer-Based Fault Diagnosis for Nonlinear Systems Using MATLAB®*. Springer, 2016.

[16] C. Edwards and C. P. Tan, "Sensor fault tolerant control using sliding mode observers," *Control Engineering Practice*, vol. 14, no. 8, pp. 897–908, 2006.

[17] C. Tan and C. Edwards, "Sensor and/or actuator fault reconstruction plays a key role in the ftc design," *Asian J Control*, vol. 9, no. 3, pp. 340–344, 2007.

[18] C. Edwards, S. K. Spurgeon, and R. J. Patton, "Sliding mode observers for fault detection and isolation," *Automatica*, vol. 36, no. 4, pp. 541–553, 2000.

[19] P. Kudva, N. Viswanadham, and A. Ramakrishna, "Observers for linear systems with unknown inputs," *IEEE Transactions on Automatic Control*, vol. 25, no. 1, pp. 113–115, 1980.

[20] H. Yang and M. Saif, "State observation, failure detection and isolation (fdi) in bilinear systems," *International Journal of Control*, vol. 67, no. 6, pp. 901–920, 1997.

[21] W. Chen and M. Saif, "Unknown input observer design for a class of nonlinear systems: an lmi approach," in *American Control Conference, 2006.* IEEE, 2006, pp. 5–pp.

[22] X. Liu and Z. Gao, "Unknown input observers for fault diagnosis in lipschitz nonlinear systems," in *Mechatronics and Automation (ICMA), 2015 IEEE International Conference on.* IEEE, 2015, pp. 1555–1560.

[23] R. Seliger and P. Frank, "Robust component fault detection and isolation in nonlinear dynamic systems using nonlinear unknown input observers," *IFAC Proceedings Volumes*, vol. 24, no. 6, pp. 277–282, 1991.

[24] M. Witczak, V. Puig, D. Rotondo, M. de Rozprza Faygel, and M. Mrugalski, "A robust observer design for unknown input nonlinear systems: Application to fault diagnosis of a wind turbine," in *Control and Automation (MED), 2015 23th Mediterranean Conference on.* IEEE, 2015, pp. 162–167.

[25] K. C. Veluvolu and Y. C. Soh, "Discrete-time sliding-mode state and unknown input estimations for nonlinear systems," *IEEE Transactions on Industrial Electronics*, vol. 56, no. 9, pp. 3443–3452, 2009.

[26] D. Wang and K.-Y. Lum, "Adaptive unknown input observer approach for aircraft actuator fault detection and isolation," *International Journal of Adaptive Control and Signal Processing*, vol. 21, no. 1, pp. 31–48, 2007.

[27] W. Chen and M. Saif, "Fault detection and isolation based on novel unknown input observer design," in *American Control Conference, 2006.* IEEE, 2006, pp. 6–pp.

[28] D. Koenig and S. Mammar, "Design of a class of reduced order unknown inputs nonlinear observer for fault diagnosis," in *American Control Conference, 2001. Proceedings of the 2001*, vol. 3. IEEE, 2001, pp. 2143–2147.

[29] H. Wang and S. Daley, "Actuator fault diagnosis: An adaptive observer-based technique," *IEEE transactions on Automatic Control*, vol. 41, no. 7, pp. 1073–1078, 1996.

[30] E. A. Garcia and P. Frank, "Deterministic nonlinear observer-based approaches to fault diagnosis: a survey," *Control Engineering Practice*, vol. 5, no. 5, pp. 663–670, 1997.

[31] B. Jiang, M. Staroswiecki, and V. Cocquempot, "Fault diagnosis based on adaptive observer for a class of non-linear systems with unknown parameters," *International Journal of Control*, vol. 77, no. 4, pp. 367–383, 2004.

[32] A. Xu and Q. Zhang, "Nonlinear system fault diagnosis based on adaptive estimation," *Automatica*, vol. 40, no. 7, pp. 1181–1193, 2004.

[33] S. Rahme and N. Meskin, "Adaptive sliding mode observer for sensor fault diagnosis of an industrial gas turbine," *Control Engineering Practice*, vol. 38, pp. 57–74, 2015.

[34] Q. Shen, B. Jiang, and P. Shi, *Fault Diagnosis and Fault-Tolerant Control Based on Adaptive Control Approach*. Springer, 2017, vol. 91.

[35] E. S. Tehrani, K. Khorasani, and S. Tafazoli, "Dynamic neural network-based estimator for fault diagnosis in reaction wheel actuator of satellite attitude control system," in *Neural Networks, 2005. IJCNN'05. Proceedings. 2005 IEEE International Joint Conference on*, vol. 4. IEEE, 2005, pp. 2347–2352.

[36] H. A. Talebi, F. Abdollahi, R. V. Patel, and K. Khorasani, *Neural network-based state estimation of nonlinear systems: application to fault detection and isolation*. Springer, 2009, vol. 395.

[37] M. Mrugalski, M. Luzar, M. Pazera, M. Witczak, and C. Aubrun, "Neural network-based robust actuator fault diagnosis for a non-linear multi-tank system," *ISA transactions*, vol. 61, pp. 318–328, 2016.

[38] M.-A. Massoumnia, "A geometric approach to the synthesis of failure detection filters," *IEEE Transactions on automatic control*, vol. 31, no. 9, pp. 839–846, 1986.

[39] C. De Persis and A. Isidori, "A geometric approach to nonlinear fault detection and isolation," *IEEE transactions on automatic control*, vol. 46, no. 6, pp. 853–865, 2001.

[40] Y. Hou, Q. Cheng, A. Qiu, and Y. Jin, "A new method of sensor fault diagnosis for under-measurement system based on space geometry approach," *International Journal of Control, Automation and Systems*, vol. 13, no. 1, pp. 39–44, 2015.

[41] N. Meskin and K. Khorasani, "Robust fault detection and isolation of time-delay systems using a geometric approach," *Automatica*, vol. 45, no. 6, pp. 1567–1573, 2009.

[42] A. Baniamerian, N. Meskin, and K. Khorasani, "A geometric approach to fault detection and isolation of multi-dimensional (nd) systems," *Multidimensional Systems and Signal Processing*, pp. 1–26, 2016.

[43] P. Baldi, M. Blanke, P. Castaldi, N. Mimmo, and S. Simani, "Combined geometric and neural network approach to generic fault diagnosis in satellite actuators and sensors," *IFAC-PapersOnLine*, vol. 49, no. 17, pp. 432–437, 2016.

[44] V. I. Utkin, "Sliding modes and their applications in variable structure systems," *Mir, Moscow*, 1978.

[45] S. Drakunov and V. Utkin, "Sliding mode observers. tutorial," in *Decision and Control, 1995., Proceedings of the 34th IEEE Conference on*, vol. 4. IEEE, 1995, pp. 3376–3378.

[46] L. Fridman, A. Levant, and J. Davila, "Observation of linear systems with unknown inputs via high-order sliding-modes," *International Journal of Systems Science*, vol. 38, no. 10, pp. 773–791, 2007.

[47] T. Floquet, C. Edwards, and S. K. Spurgeon, "On sliding mode observers for systems with unknown inputs," *International Journal of Adaptive Control and Signal Processing*, vol. 21, no. 8-9, pp. 638–656, 2007.

[48] C. P. Tan and C. Edwards, "Sliding mode observers for robust detection and reconstruction of actuator and sensor faults," *International Journal of Robust and Nonlinear Control*, vol. 13, no. 5, pp. 443–463, 2003.

[49] S. K. Spurgeon, "Sliding mode observers: a survey," *International Journal of Systems Science*, vol. 39, no. 8, pp. 751–764, 2008.

[50] W. Chen and M. Saif, "Robust fault detection and isolation in constrained nonlinear systems via a second order sliding mode observer," *IFAC Proceedings Volumes*, vol. 35, no. 1, pp. 269–274, 2002.

[51] X.-G. Yan and C. Edwards, "Nonlinear robust fault reconstruction and estimation using a sliding mode observer," *Automatica*, vol. 43, no. 9, pp. 1605–1614, 2007.

[52] W. Chen, Q. Wu, E. Tafazzoli, and M. Saif, "Actuator fault diagnosis using high-order sliding mode differentiator (hosmd) and its application to a laboratory 3d crane," *IFAC Proceedings Volumes*, vol. 41, no. 2, pp. 4809–4814, 2008.

[53] K. Veluvolu and Y. Soh, "Fault reconstruction and state estimation with sliding mode observers for lipschitz non-linear systems," *IET control theory & applications*, vol. 5, no. 11, pp. 1255–1263, 2011.

[54] J. Zhang, A. K. Swain, and S. K. Nguang, "Detection and isolation of incipient sensor faults for a class of uncertain non-linear systems," *IET Control Theory & Applications*, vol. 6, no. 12, pp. 1870–1880, 2012.

[55] M. Du, J. Scott, and P. Mhaskar, "Actuator and sensor fault isolation of nonlinear process systems," *Chemical Engineering Science*, vol. 104, pp. 294–303, 2013.

[56] X. Zhang, M. M. Polycarpou, and T. Parisini, "A robust detection and isolation scheme for abrupt and incipient faults in nonlinear systems," *IEEE transactions on automatic control*, vol. 47, no. 4, pp. 576–593, 2002.

[57] H. Wang, Z. J. Huang, and S. Daley, "On the use of adaptive updating rules for actuator and sensor fault diagnosis," *Automatica*, vol. 33, no. 2, pp. 217–225, 1997.

[58] C. P. Tan and C. Edwards, "Sliding mode observers for reconstruction of simultaneous actuator and sensor faults," in *Decision and Control, 2003. Proceedings. 42nd IEEE Conference on*, vol. 2. IEEE, 2003, pp. 1455–1460.

[59] R. Raoufi and H. Marquez, "Simultaneous sensor and actuator fault reconstruction and diagnosis using generalized sliding mode observers," in *American Control Conference (ACC), 2010*. IEEE, 2010, pp. 7016–7021.

[60] J. Zhang, A. K. Swain, and S. K. Nguang, "Simultaneous robust actuator and sensor fault estimation for uncertain non-linear lipschitz systems," *IET Control Theory & Applications*, vol. 8, no. 14, pp. 1364–1374, 2014.

[61] M. L. McIntyre, W. E. Dixon, D. M. Dawson, and I. D. Walker, "Fault identification for robot manipulators," *IEEE Transactions on Robotics*, vol. 21, no. 5, pp. 1028–1034, 2005.

[62] Q. Wu and M. Saif, "Neural adaptive observer based fault detection and identification for satellite attitude control systems," in *American Control Conference, 2005. Proceedings of the 2005*. IEEE, 2005, pp. 1054–1059.

[63] G. Paviglianiti, F. Pierri, F. Caccavale, and M. Mattei, "Robust fault detection and isolation for proprioceptive sensors of robot manipulators," *Mechatronics*, vol. 20, no. 1, pp. 162–170, 2010.

[64] B. Halder and N. Sarkar, "Robust fault detection of a robotic manipulator," *The International Journal of Robotics Research*, vol. 26, no. 3, pp. 273–285, 2007.

[65] C. T. Trung, H. M. Son, D. P. Nam, T. N. Long, P. A. Viet *et al.*, "Fault detection and isolation for robot manipulator using statistics," in *System Science and Engineering (ICSSE), 2017 International Conference on.* IEEE, 2017, pp. 340–343.

[66] D. Brambilla, L. M. Capisani, A. Ferrara, and P. Pisu, "Fault detection for robot manipulators via second-order sliding modes," *IEEE Transactions on Industrial Electronics*, vol. 55, no. 11, pp. 3954–3963, 2008.

[67] W. Chen and M. Saif, "Observer-based fault diagnosis of satellite systems subject to time-varying thruster faults," *Journal of dynamic systems, measurement, and control*, vol. 129, no. 3, pp. 352–356, 2007.

[68] H.-J. Ma and G.-H. Yang, "Simultaneous fault diagnosis for robot manipulators with actuator and sensor faults," *Information Sciences*, vol. 366, pp. 12–30, 2016.

[69] H. Alwi and C. Edwards, "Fault tolerant control using sliding modes with on-line control allocation," *Automatica*, vol. 44, no. 7, pp. 1859–1866, 2008.

[70] H. Ríos, S. Kamal, L. M. Fridman, and A. Zolghadri, "Fault tolerant control allocation via continuous integral sliding-modes: a hosm-observer approach," *Automatica*, vol. 51, pp. 318–325, 2015.

[71] M. Marwaha and J. Valasek, "Fault-tolerant control allocation for mars entry vehicle using adaptive control," *International Journal of Adaptive Control and Signal Processing*, vol. 25, no. 2, pp. 95–113, 2011.

[72] Q. Hu, B. Li, D. Wang, and E. Kee Poh, "Velocity-free fault-tolerant control allocation for flexible spacecraft with redundant thrusters," *International Journal of Systems Science*, vol. 46, no. 6, pp. 976–992, 2015.

[73] H. Noura, D. Sauter, F. Hamelin, and D. Theilliol, "Fault-tolerant control in dynamic systems: Application to a winding machine," *IEEE control systems*, vol. 20, no. 1, pp. 33–49, 2000.

[74] J. Lan and R. J. Patton, "A new strategy for integration of fault estimation within fault-tolerant control," *Automatica*, vol. 69, pp. 48–59, 2016.

[75] X. Zhang, T. Parisini, and M. M. Polycarpou, "Adaptive fault-tolerant control of nonlinear uncertain systems: an information-based diagnostic approach," *IEEE Transactions on automatic Control*, vol. 49, no. 8, pp. 1259–1274, 2004.

[76] Z. Gao and S. X. Ding, "Actuator fault robust estimation and fault-tolerant control for a class of nonlinear descriptor systems," *Automatica*, vol. 43, no. 5, pp. 912–920, 2007.

[77] B. Jiang, M. Staroswiecki, and V. Cocquempot, "Fault accommodation for nonlinear dynamic systems," *IEEE Transactions on Automatic Control*, vol. 51, no. 9, pp. 1578–1583, 2006.

[78] F. Chen, W. Lei, G. Tao, and B. Jiang, "Actuator fault estimation and reconfiguration control for the quad-rotor helicopter," *International Journal of Advanced Robotic Systems*, vol. 13, no. 1, p. 33, 2016.

[79] M. Sami and R. J. Patton, "Active fault tolerant control for nonlinear systems with simultaneous actuator and sensor faults," *International Journal of Control, Automation and Systems*, vol. 11, no. 6, pp. 1149–1161, 2013.

[80] K. Zhang, B. Jiang, X.-G. Yan, and Z. Mao, "Adaptive robust fault-tolerant control for linear mimo systems with unmatched uncertainties," *International Journal of Control*, vol. 90, no. 10, pp. 2253–2269, 2017.

[81] X. Tang, G. Tao, and S. M. Joshi, "Adaptive output feedback actuator failure compensation for a class of non-linear systems," *International Journal of Adaptive Control and Signal Processing*, vol. 19, no. 6, pp. 419–444, 2005.

[82] A.-M. Zou and K. D. Kumar, "Adaptive fuzzy fault-tolerant attitude control of spacecraft," *Control Engineering Practice*, vol. 19, no. 1, pp. 10–21, 2011.

[83] Q. Yang, S. S. Ge, and Y. Sun, "Adaptive actuator fault tolerant control for uncertain nonlinear systems with multiple actuators," *Automatica*, vol. 60, pp. 92–99, 2015.

[84] Z. Shen, Y. Ma, and Y. Song, "Robust adaptive fault-tolerant control of mobile robots with varying center of mass," *IEEE Transactions on Industrial Electronics*, 2017.

[85] R. J. Patton, "Fault-tolerant control," *Encyclopedia of systems and control*, pp. 422–428, 2015.

[86] B. Liang and G. Duan, "Robust h-infinity fault-tolerant control for uncertain descriptor systems by dynamical compensators," *Journal of Control Theory and Applications*, vol. 2, no. 3, pp. 288–292, 2004.

[87] M. Gholami, V. Cocquempot, H. Schiøler, and T. Bak, "Passive fault tolerant control of piecewise affine systems based on h infinity synthesis," *IFAC Proceedings Volumes*, vol. 44, no. 1, pp. 3084–3089, 2011.

[88] Y. Wang, C. Tan, and X. Zhang, "Robust fault-tolerant h control for uncertain descriptor systems by dynamical compensators," in *Control and Decision Conference (CCDC), 2010 Chinese*. IEEE, 2010, pp. 50–55.

[89] R. Zhang, J. Qiao, T. Li, and L. Guo, "Robust fault-tolerant control for flexible spacecraft against partial actuator failures," *Nonlinear Dynamics*, vol. 76, no. 3, pp. 1753–1760, 2014.

[90] M. Davoodi, A. Golabi, H. Talebi, and H. Momeni, "Simultaneous fault detection and control design for switched linear systems based on dynamic observer," *Optimal Control Applications and Methods*, vol. 34, no. 1, pp. 35–52, 2013.

[91] L.-Y. Hao and G.-H. Yang, "Robust fault tolerant control based on sliding mode method for uncertain linear systems with quantization," *ISA transactions*, vol. 52, no. 5, pp. 600–610, 2013.

[92] H. Lee and Y. Kim, "Fault-tolerant control scheme for satellite attitude control system," *IET control theory & applications*, vol. 4, no. 8, pp. 1436–1450, 2010.

[93] M. Moradi and A. Fekih, "A stability guaranteed robust fault tolerant control design for vehicle suspension systems subject to actuator faults and disturbances," *IEEE Transactions on Control Systems Technology*, vol. 23, no. 3, pp. 1164–1171, 2015.

[94] M. Van, S. S. Ge, and H. Ren, "Finite time fault tolerant control for robot manipulators using time delay estimation and continuous nonsingular fast terminal sliding mode control," *IEEE transactions on cybernetics*, vol. 47, no. 7, pp. 1681–1693, 2017.

[95] C.-C. Peng and C.-L. Chen, "Sliding mode control framework for reconstruction and rejection of mismatched and matched disturbances," in *Control Conference (ECC), 2009 European*. IEEE, 2009, pp. 2905–2910.

[96] B. Tamhane, A. Mujumdar, and S. Kurode, "Mismatched disturbance compensation using sliding mode control," in *Control Conference (ASCC), 2015 10th Asian*. IEEE, 2015, pp. 1–6.

[97] M. W. Spong, S. Hutchinson, and M. Vidyasagar, *Robot modeling and control*. Wiley New York, 2006, vol. 3.

[98] J. Petrich and D. J. Stilwell, "Robust control for an autonomous underwater vehicle that suppresses pitch and yaw coupling," *Ocean Engineering*, vol. 38, no. 1, pp. 197–204, 2011.

[99] T. I. Fossen, *Marine control systems: guidance, navigation and control of ships, rigs and underwater vehicles*. Marine Cybernetics, 2002.

[100] K. S. Narendra and A. M. Annaswamy, *Stable adaptive systems*. Courier Corporation, 2012.

[101] J. J. Craig, *Introduction to robotics: mechanics and control*. Pearson Prentice Hall Upper Saddle River, 2005, vol. 3.

[102] R. V. Patel, H. A. Talebi, J. Jayender, and F. Shadpey, "A robust position and force control strategy for 7-dof redundant manipulators," *IEEE/ASME Transactions on Mechatronics*, vol. 14, no. 5, pp. 575–589, 2009.

[103] T. I. Fossen, *Guidance and control of ocean vehicles*. John Wiley & Sons Inc, 1994.